Microbial dormancy and its impacts on northern temperate and boreal terrestrial ecosystem carbon budget

Junrong Zha and Qianlai Zhuang

Department of Earth, Atmospheric, and Planetary Sciences and Department of Agronomy, Purdue University, West Lafayette, IN 47907 USA

Submitted to: *Biogeoscience*

Correspondence to: qzhuang@purdue.edu

Abstract

A large amount of soil carbon in northern temperate and boreal regions could be emitted as greenhouse gases in a warming future. However, lacking detailed microbial processes such as microbial dormancy in current biogeochemistry models might have biased the quantification of the regional carbon dynamics. Here the effect of microbial dormancy was incorporated into a biogeochemistry model to improve the quantification for the last and this century. Compared with the previous model without considering the microbial dormancy, the new model estimated the regional soils stored 75.9 Pg more C in the terrestrial ecosystems during the last century, and will store 50.4 Pg and 125.2 Pg more C under the RCP 8.5 and RCP 2.6 scenarios, respectively, in this century. This study highlights the importance of the representation of microbial dormancy in earth system models to adequately quantify the carbon dynamics in the northern temperate and boreal natural terrestrial ecosystems.

1. Introduction

The land ecosystems in northern temperate and boreal regions (>45 ºN) occupy 22% of the global surface and store over 40% of the global soil organic carbon (SOC) (McGuire & Hobbie, 1997; Melillo et al., 1993; Tarnocai et al., 2009; Hugelius et al., 2014). During the past decades, a greening accompanying a warming in the region has been documented (Zhou et al., 2001; Lloyd et al., 2002; Stow et al., 2004; Callaghan et al., 2005; Tape et al., 2006). The regional carbon dynamics are expected to loom large in the global carbon cycle and exert large feedbacks to the global climate system (McGuire et al., 2009; Davidson & Janssens, 2006; Bond-Lamberty & Thomson, 2010).

To date, numerous ecosystem models have been developed to project the feedbacks between terrestrial ecosystem carbon cycling and climate (Raich et al., 1991; Zhuang et al., 2001, 2002, 2015; Parton et al., 1993; Knorr et al., 2005; Running & Coughlan, 1988), but they can bias their quantifications due to missing detailed microbial mechanisms in these models (Schmidt et al., 2011; Todd-Brown et al., 2013; Conant et al., 2011; Treseder et al., 2011). Microorganisms play a central role in decomposition of litter and soil organic carbon, which further governs the global carbon cycling and climate change (Xu et al., 2014; Treseder et al., 2011; Wang et al., 2015). An emerging field of research has begun to incorporate microbial ecology into existing process-based models to represent decomposition in ways that include important microbial processes that were previously ignored (Zha & Zhuang, 2018; Schimel & Weintraub, 2003; Allison et al., 2010; German et al., 2012). These microbial-based models tend to better reproduce field and satellite observations than traditional ones that treat soil decomposition as a first-order decay process without considering microbial activities (Treseder et al., 2011; Wieder et al., 2013; Todd-Brown et al., 2011; Lawrence et al., 2009; Moorhead et

al., 2006). However, some vital microbial traits such as microbial dormancy and community shifts are still rarely explicitly considered in large-scale ecosystem models (Wieder et al., 2015), and this may introduce notable uncertainties (Graham et al., 2014, 2016; Wang et al., 2015; Bouskill et al., 2012; Kaiser et al., 2014).

Dormancy is broadly recognized as a strategy for microorganisms to cope with periodical environmental stresses (Harder & Dijkhuizen, 1983). When environmental conditions are unfavorable for growth, microbes switch to a dormant state, which is a reversible state of low to zero metabolic activity (Stolpovsky et al., 2011; Lennon & Jones, 2011). In this state, biogeochemical processes such as soil decomposition are slow (Blagodatskaya et al., 2013). At any given time, there is only a fraction of, likely below 50%, metabolically active microbes in natural soils (Wang et al., 2015; Stolpovsky et al., 2011). Soil decomposition and nutrient cycling mainly depend on these active microbes because only active ones can consume organic matter and replicate themselves (Wang et al., 2015; Blagodatskaya et al., 2014). To date, most existing biogeochemistry models use total rather than active microbial biomass as an indicator of microbial activities (Wieder et al., 2015), which could bias the estimates of soil decomposition and ecosystem carbon budget (Hagerty et al., 2014; He et al., 2015). Especially, the northern temperate and boreal terrestrial ecosystems are nitrogen-limited, neglecting microbial dormancy will lead to incorrect estimates of nitrogen availability through soil decomposition, failing to capture nitrogen feedbacks to carbon dynamics (Wang et al., 2015; Stolpovsky et al., 2011; Thullner et al., 2005). Furthermore, these ecosystems have experienced a marked seasonality of active and dormant microbial cycles and the above-global-average warming, which might have increased the proportion of active microbes in soils (He et al., 2015). Thus, incorporating

dormancy effects will improve model realism to provide a better projection of the northern temperate and boreal terrestrial ecosystem carbon dynamics.

This study incorporated the effects of microbial dormancy trait into an extant process-based biogeochemistry model (MIC-TEM) (Zha & Zhuang, 2018; He et al., 2015). The dormant and active microbial physiology has been considered explicitly in the new version of model (MIC-TEM-dormancy). The revised model was parameterized, validated, and then applied to evaluate the carbon dynamics during the last and this centuries in the northern temperate and boreal terrestrial ecosystems (north 45 ºN above). By comparing the results of MIC-TEM-dormancy and MIC-TEM, we can show that incorporating microbial dormancy may produce a much different prediction in historical and future carbon budget.

2. Methods

2.1 Overview

Due to the importance of microbial dormancy, some recent work has been done to consider the metabolic activation and deactivation of microbes in soil and its effects on soil carbon (C) dynamics and climate feedbacks. For example, Wang et al. (2015) has incorporated transformation processes between active and dormant states to develop two versions of MEND, that is, MEND with and without dormancy. The two versions of the model have been applied to quantify the carbon decomposition in laboratory incubations of four soils. Salazar et al. (2018) have also taken microbial dormancy into account to compare their predictions of microbial biomass and soil heterotrophic respiration (R_H) under simulated cycles of stressful (dryness) and favorable (wet pulses) conditions. Our study extends those modeling studies to the northern temperate and boreal terrestrial ecosystems by developing a more detailed biogeochemistry model considering the

144 dormancy impacts. Below, we first describe how we developed the new model (MIC-TEM-
145 dormancy) by incorporating the microbial dormancy trait into an existing microbial-based
146 biogeochemistry model (MIC-TEM)**.** Second, we discuss how parameterization and validation of
147 MIC-TEM-dormancy model were conducted using observed net ecosystem exchange data, and
148 heterotrophic respiration data at representative sites. Third, we presented how the model was
149 applied to natural ecosystems in the region (above 45 ºN) for the 20th and 21st centuries and
150 discussed the dormancy effects on their regional carbon budget.
151
152 **2.2 Model description**
153 A non-dormancy version of biogeochemistry model (MIC-TEM) has been developed by
154 incorporating a microbial module (Allison et al., 2010) into an extant large-scale biogeochemical
155 model (TEM) to explicitly (Zhuang et al., 2003) consider the effects of microbial dynamics and
156 enzyme kinetics on carbon dynamics (Zha & Zhuang, 2018). Here we further advanced the MIC-
157 TEM by incorporating algorithms that describe the effects of microbial dormancy dynamics
158 based on He et al. (2015). Different from He et al. (2015), in which microbial module was driven
159 with existing data of carbon stocks and fluxes, our study incorporated the microbial module into
160 an extant MIC-TEM that simulates carbon data dynamically. This coupling enables us to
161 extrapolate our model to northern temperate and boreal terrestrial ecosystems, rather than only
162 for temperate forest region in He et al. (2015). In our new model (MIC-TEM-dormancy),
163 microbial biomass pool was divided into two fractions, including the dormant and active
164 microbial biomass pools. The two microbial biomass pools and the reversible transition between
165 them have been considered explicitly in the new model (Figure 1), which was ignored in MIC-
166 TEM.

In previous MIC-TEM, heterotrophic respiration (R_H) is simply calculated as the product of ASSIM and CUE, which are microbial assimilation and carbon use efficiency, respectively. For detailed carbon dynamics in MIC-TEM, see Zha & Zhuang (2018).

Here we revised MIC-TEM by incorporating microbial dormancy dynamics according to He et al. (2015). In MIC-TEM-dormancy, the soil heterotrophic respiration R_H is revised to include three parts: the maintenance respiration from the active and dormant microorganisms and the CO_2 production through the process of microbial assimilation (He et al., 2015):

$$R_H = m_R Q_{10mic}^{\frac{temp-15}{10}} B_a + \beta m_R Q_{10mic}^{\frac{temp-15}{10}} B_d + CO_2 \quad (1)$$

where the first two terms are maintenance respiration from the active and dormant microorganisms, respectively. The last term is the CO_2 produced during the process of microbial assimilation.

For first two terms, B_a and B_d represents the active and dormant microbial biomass pool, respectively. The parameter m_R denotes the specific maintenance rate at active state (h^{-1}), and β is the ratio of dormant maintenance rate to active maintenance rate. Thus, βm_R denotes the maximum specific maintenance rate at dormant state. Temperature sensitivity was expressed as the Q_{10} function ($Q_{10}^{\frac{temp-15}{10}}$), where temp is soil temperature at top 20 cm (units: ℃).

For the third term, the CO_2 produced through microbial assimilation is calculated as in He et al. (2015) and Allison et al. (2010):

$$CO_2 = ASSIM \times (1-Y_g) \quad (2)$$

Where ASSIM represents the microbial assimilation and the parameter Y_g represents carbon use efficiency. Microbial assimilation (ASSIM) is calculated as in He et al. (2015):

$$ASSIM = \frac{1}{Y_g} \frac{\Phi}{\alpha} m_R Q_{10enz}^{\frac{temp-15}{10}} Ba \left(\frac{CN_{soil}}{CN_{mic}}\right)^{0.6} \quad (3)$$

189 Here parameter α is maintenance weight (h^{-1}), CN_{soil} and CN_{mic} denotes the C:N ratios of soil and
190 that of microbial biomass. Besides, Φ is the substrate saturation level and defined as in He et al.
191 (2015) and Wang et al. (2014):

192 $$\Phi = \frac{S}{K_s + S} \quad (4)$$

193 Where K_s is the half saturation constant for substrate uptake as indicated by the Michaelis–Menten
194 kinetic, and S is soluble C substrates that are directly accessible for microbial assimilation (Wang
195 et al., 2014). Here we quantified concentration of soluble C substrates that are directly accessible
196 for microbial assimilation by using conceptual framework from Davidson et al. (2012):

197 $$S = \text{Soluble C} \times D_{liq} \times \theta^3 \quad (5)$$

198 The term 'Soluble C' denotes the state variable of soluble carbon pool. D_{liq} is the diffusion
199 coefficient of the substrate in the liquid phase, and is formulated as:

200 $$D_{liq} = 1/(1\text{-}BD/PD)^3 \quad (6)$$

201 Where BD is the bulk density and PD is the soil particle density. θ is the volumetric soil moisture.
202 Different from MIC-TEM, the transitions between active and dormant microbial biomass are
203 included in MIC-TEM-dormancy.

204 $$B_{a\to d} = (1 - \Phi) m_R Q_{10mic}^{\frac{temp-15}{10}} B_a \quad (7)$$

205 $$B_{d\to a} = \Phi m_R Q_{10mic}^{\frac{temp-15}{10}} B_d \quad (8)$$

206 Where $B_{a\to d}$ and $B_{d\to a}$ denote the transition from the active to dormant microbe and from the
207 dormant to active microbe, respectively (He et al., 2015; Wang et al., 2014). Thus, dormancy rate
208 is affected by active and dormant biomass, soil temperature (temp) and soil moisture (θ in Φ).
209 The active microbial biomass (B_a) is modeled as (He et al., 2015; Wang et al., 2014):

210 $$\frac{dBa}{dt} = ASSIM \times Y_g - m_R Q_{10mic}^{\frac{temp-15}{10}} B_a - B_{a\to d} + B_{d\to a} - DEATH - EPROD \quad (9)$$

Where DEATH and EPROD denotes microbial biomass death and enzyme production, which are modeled as proportional to active microbial biomass with constant rates r_{death} and $r_{EnzProd}$ (Allison et al., 2010):

$$DEATH = r_{death} \times Ba \quad (10)$$

$$EPROD = r_{EnzProd} \times Ba \quad (11)$$

Where r_{death} and $r_{EnzProd}$ are the rate constants of microbial death and enzyme production, respectively.

The dormant microbial biomass (B_d) is modeled as (He et al., 2015; Wang et al., 2014):

$$\frac{dB_d}{dt} = -\beta m_R Q_{10mic}^{\frac{temp-15}{10}} B_d + B_{a\to d} - B_{d\to a} \quad (12)$$

The Soluble C pool is modeled as (He et al., 2015; Allison et al., 2010):

$$\frac{d\ Soluble\ C}{dt} = DECAY - ASSIM + ELOSS + DEATH \quad (13)$$

Where DECAY represents the enzymatic decay of soil organic carbon (SOC), and ELOSS represents the loss of enzyme.

DECAY is regulated by enzyme biomass (ENZ), soil organic carbon (SOC), soil temperature, and substrate quality (He et al., 2015):

$$DECAY = V_{max} \times Q_{10enz}^{\frac{temp-15}{10}} \times ENZ \times \frac{SOC}{Km_{uptake}+SOC} \times (120 - CN_{soil}) \quad (14)$$

Where V_{max} is the maximum SOC decay rate, Km_{uptake} is half saturation constant for enzymatic decay.

ELOSS is modeled as a first-order process (Allison et al., 2010) to represent enzyme turnover:

$$ELOSS = r_{enzloss} \times ENZ \quad (15)$$

Where $r_{enzloss}$ is the rate constant of enzyme loss.

The soil organic carbon pool (SOC) is modeled as:

$$\frac{dSOC}{dt} = \text{Litterfall} - \text{DECAY} \quad (16)$$

Where Litterfall is estimated as a function of vegetation carbon (Zhuang et al., 2010).

Last, enzyme pool (ENZ) is modeled as:

$$\frac{dENZ}{dt} = \text{EPROD-ELOSS} \quad (17)$$

With the modification of microbial carbon dynamics by considering microbial life-history trait, soil decomposition is changed since it is controlled by microbes. When microbial dormancy is considered, the number of active microbes that participate in soil decomposition is much less. The changes in soil decomposition directly influence the amount of soil respiration, and further influence soil nitrogen (N) mineralization that determines soil N availability for plants, affecting gross primary production (GPP). Since both GPP and R_H can be affected by microbial dormancy, net ecosystem production (NEP) will also be affected.

2.3 Model parameterization and validation

The detailed description of parameters that are related to microbial dormancy can be found in He et al. (2015) (Table 1). Here we calibrated the MIC-TEM-dormancy at six representative sites with gap-filled monthly net ecosystem productivity (NEP, $gCm^{-2}mon^{-1}$) data in northern temperate and boreal regions (Table 2). Site-level climatic data and soil texture data were organized for driving model. All sites information can be found on AmeriFlux network (Davidson et al., 2000). The results for model parameterization were presented in Figure 2. We conducted the parameterization using a global optimization algorithm known as SCE-UA (Shuffled complex evolution) method (Duan et al., 1994). An ensemble of 50 independent sets of parameters were performed based on prior ranges from literature (Table 1) to minimize the difference between the

255 monthly simulated and measured NEP at the chosen sites. The cost function of the minimization
256 is:

257 $$\mathrm{Obj} = \sum_{i=1}^{k}(\mathrm{NEP}_{obs,i} - \mathrm{NEP}_{sim,i})^2 \quad (18)$$

258 Where $\mathrm{NEP}_{obs,i}$ and $\mathrm{NEP}_{sim,i}$ are the observed and simulated NEP, respectively. k is the number of
259 data pairs for comparison. Except for the parameters of microbial dormancy, other parameters are
260 derived directly from MIC-TEM (Zha & Zhuang, 2018). The optimized parameters were used for
261 model validation and regional simulations.

262 For model validation, we chose another six sites that containing monthly NEP data from
263 AmeriFlux network (Table 3). Four of these six sites were also used for parameterization (Table
264 2). However, we used the data of different observation periods for model validation for those
265 overlapped sites. Moreover, we also conducted site-level validations with monthly soil respiration
266 data from AmeriFlux network and Fluxnet dataset. The site information was provided in Table 4.
267 For these sites, we assumed 50% of soil respiration was heterotrophic respiration (R_H) for forest
268 (Hanson et al., 2000), 60% and 70% of that was R_H for grassland (Wang et al., 2009) and tundra
269 (Billings et al., 1977). Because there is a limited amount of available RH data, we could not
270 conduct a regional validation for all pixels in northern temperate and boreal regions. Instead, we
271 extracted 61 sites providing data of average annual heterotrophic respiration from ORNL global
272 Soil Respiration Dataset (https://daac.ornl.gov/SOILS/guides/SRDB_V4.html, Bond-Lamberty et
273 al., 2018) for model validation. The site-level observed average annual R_H was used to compare
274 with simulated annual R_H by MIC-TEM-dormancy and MIC-TEM. The MIC-TEM-dormancy was
275 run at monthly time step to keep consistent with the time step of MIC-TEM. Although microbial
276 dynamics occur at fine temporal scales (Tang & Riley, 2014), we can still quantify the cumulative

impacts of microbial dynamics on carbon and nitrogen cycling at monthly time by not changing the model structure.

2.4 Spatial extrapolation

For historical simulations during the 20th century, two sets of regional simulations using MIC-TEM-dormancy and MIC-TEM at a spatial resolution of 0.5° latitude × 0.5° longitude were conducted. Our model simulation contains two parts: spin-up and transient simulation. A typical spin-up was conducted to get the model to a steady state for each spatial location, which will be used as initial conditions for transient simulations (McGuire et al., 1992). During spin-up procedure, cyclic forcing data was used to force the model run, and repeated continuously until dynamic equilibrium was achieved at which the modeled state variables show a cyclic pattern or become constant. Specifically, this study used the monthly historical climate data from 1900 to 1940 to repeatedly drive the model for the spin-up. Before spin-up procedure, the model was initialized with default built-in carbon stocks (Raich et al., 1991). During transient simulations, the calibrated ecosystem-specific parameters were used for regional simulations. The previous dynamic equilibrium was used as initial value for transient simulation. The historical climatic forcing data, including the monthly air temperature, precipitation, cloudiness, and atmospheric CO_2 concentrations, were organized from the Climatic Research Unit (CRU TS3.1) from the University of East Anglia (Harris et al., 2014). We also used gridded data of soil texture (Zhuang et al., 2003), elevation (Zhuang et al., 2015), and potential natural vegetation (Melillo et al., 1993) from literatures. In our model, we assumed that soil texture, elevation, and potential natural vegetation data only vary spatially, not vary over time (Zhuang et al., 2015).

In addition, regional simulations over the 21st century were conducted under two Intergovernmental Panel on Climate Change (IPCC) climate scenarios (RCP 2.6 and RCP 8.5). The future climatic forcing data under these two climate change scenarios were derived from the HadGEM2-ESmodel, which is a member of CMIP5project213 (https://esgf-node.llnl.gov/search/cmip5/). Then the regional estimations were obtained by summing up the gridded outputs for our study region. The positive simulated NEP represents a CO_2 sink from the atmosphere to terrestrial ecosystems, while a negative value represents a source of CO_2 from terrestrial ecosystems to the atmosphere.

2.5 Parameter equifinality effects

Our previous studies using TEM has demonstrated that equifinality derived from site-level parameterization will affect the uncertainty in the estimation of regional carbon dynamics (Tang and Zhuang, 2008, 2009). Here equifinality refers to that a number of sets of parameters result in model simulations that all match the data similarly well. To quantify this effect on our simulation uncertainty, we conducted ensemble regional simulations with 50 sets of parameters for both historical and future studies. The 50 sets of parameters were obtained according to the method in Tang and Zhuang (2008).

3. Results

3.1 Inversed Model Parameters and model validation

Using SCE-UA ensemble method, 50 independent sets of parameters were converged to minimize the objective function. Then the optimized parameters are calculated as the mean of these 50 sets of inversed parameters. The boxplot of parameter posterior distributions reflects different

ecosystem properties at these sites (Figure 3). For instance, growth yield was higher in tundra types than in forests, meaning microorganisms in environment with higher energy limitation tend to enhance the efficiency of energy transportation. Besides, alpha, the maintenance weight, was also higher in tundra types than in forests. From the plot for parameter beta, the ratio of dormant maintenance rate to specific maintenance rate for active biomass in tundra types is lower than that in forest types. Other microbial related parameters did not differentiate much among different vegetation types.

After parameterization, the MIC-TEM-dormancy was validated with monthly NEP data for six representative ecosystems, and the comparisons between monthly observed NEP and simulated NEP were presented in Figure 4. With the optimized parameters, the dormancy-based model was used to reproduce NEP to compare with the measured NEP (Table 5). The R^2 ranges from 0.67 for Atqasuk to 0.93 for Bartlett Experimental Forest (Table 5). Generally, our new model performs better for forest ecosystems than for tundra ecosystems. Compared with MIC-TEM, dormancy model performs better for alpine tundra, temperate coniferous forest, and grassland. For other sites, both models show similar performance (Table 5). Besides, a set of monthly soil respiration data were selected to evaluate the estimated R_H. The comparisons between monthly observed R_H and simulated R_H from two contrasting models were conducted (Figure 5). MIC-TEM-dormancy has higher R^2 and lower root mean square error (RMSE) (Table 6). Sixty-one sites with average annual R_H in northern temperate and boreal regions were used to further evaluate the new model performance. The dormancy model has lower intercept and slope with R^2 of 0.45, while R^2 of MIC-TEM is 0.3 (Figure 6). These analyses indicate that new model is more realistic in representing R_H by considering microbial dormancy.

3.2 Regional carbon dynamics during the 20th century

Regional extrapolation with both models estimated a regional terrestrial ecosystem carbon sink but with different magnitudes (Figure 7c). With optimized parameters, MIC-TEM estimated a regional carbon sink of 77.6 Pg with the interannual standard deviation of 0.21 Pg C yr^{-1} during the 20th century. However, MIC-TEM-dormancy nearly doubles the sink at 153.5 Pg with the interannual standard deviation of 0.12 Pg C yr^{-1} during the last century (Figure 7c). At the end of the century, MIC-TEM estimated that NEP reaches 1.0 Pg C yr^{-1} in comparison with MIC-TEM-dormancy estimates of 1.5 Pg C yr^{-1} (Figure 7c). Both models simulated similar trends for regional NPP, R_H and NEP (Figure 7). Generally, they show an increasing trend in the 20th century (Figure 7). Meanwhile, with optimized parameters, MIC-TEM-dormancy estimated NPP and R_H at 7.94 Pg C yr^{-1} and 6.4 Pg C yr^{-1}, which are 5.8% and 16.3% less than the estimations from MIC-TEM, respectively (Figures 7a and 7b). This pronounced difference of NEP between two models comes from the disparity between the simulated NPP and R_H with them since NEP is calculated as the difference between NPP and R_H. Without considering dormancy, MIC-TEM estimates more active microbial biomass, hence overestimating both R_H and NPP (due to higher simulated N mineralization and uptake by plants), but resulting in lower NEP than that calculated by MIC-TEM-dormancy.

Temporally, both models projected higher NPP and R_H in summer than in winter (Figures 8a and 8b) due to higher soil temperature and moisture (McGuire et al., 1992). Setting the R_H projection from MIC-TEM as a baseline, MIC-TEM-dormancy projected 33% less R_H in summer (May to September), and 30% more in winter (other months) (Figure 8b), indicating that without dormancy, model tends to estimate lower soil respiration due to ignorance of dormant respiration in winter, but higher soil respiration due to higher active biomass in summer. NEP seasonality

estimated with two models are close to each other (Figure 8c), but the dormancy model projected slightly higher NEP in summer.

3.3 Regional carbon dynamics during the 21st century

Under the RCP 8.5 scenario, both models estimated the regional natural terrestrial ecosystems act as a carbon sink (Figure 9). The MIC-TEM-dormancy predicted a C accumulation of 129.9 Pg by the end of this century. with the interannual standard deviation of 0.13 Pg C yr^{-1}, whereas MIC-TEM estimates a C accumulation of 79.5 Pg with the interannual standard deviation of 0.37 Pg C yr^{-1} during the 21st century (Figure 9). Thus, MIC-TEM-dormancy estimates an increase of 50.4 Pg regional carbon sequestration relative to MIC-TEM, with less interannual variation (Figure 9). Under this scenario, both models predict similar temporal trends for NEP, namely increasing from the 2000s and then decreasing from the 2070s onward (Figure 9). MIC-TEM-dormancy predicts that carbon sink reaches 1.36 Pg C yr^{-1} in the 2090s, which is 0.26 Pg C yr^{-1} more than projection of MIC-TEM. Moreover, MIC-TEM-dormancy estimated NPP and R_H at 10.2 Pg C yr^{-1} and 8.9 Pg C yr^{-1}, which are 1.3 Pg C yr^{-1} and 1.8 Pg C yr^{-1} less than the estimations from MIC-TEM, respectively (Figure 9).

Under the RCP 2.6 scenario, the cumulative NEP from two models diverged by 125.2 Pg C by 2100. The trajectory of inter-annual NEP estimated with the two models also diverged. The MIC-TEM predicted the region fluctuates between carbon sinks and sources, and totally acts as a carbon source of 1.6 Pg C with the interannual standard deviation of 0.24 Pg C yr^{-1} during the 21st century. In contrast, MIC-TEM-dormancy projected the region acts as a carbon sink of 123.6 Pg C with an interannual standard deviation of 0.1 Pg C yr^{-1} (Figure 9). MIC-TEM-dormancy estimates NPP and R_H at 9.9 Pg C yr^{-1} and 8.7 Pg C yr^{-1}, which are 0.5 Pg C yr^{-1} and 1.7 Pg C yr^{-}

391 ^{1} less than the estimations from MIC-TEM, respectively (Figure 9). Moreover, simulations under
392 the two contrasting climate scenarios (RCP 2.6 and RCP 8.5) exhibit a large difference of 81.1
393 Pg C of cumulative NEP during the 21st century by MIC-TEM, but only 6.3 Pg C of that by
394 MIC-TEM-dormancy.

395 MIC-TEM-dormancy estimated higher R_H in winter, but lower R_H in summer under both
396 future scenarios in the 2090s (Figure 10). NPP is the same in winter with or without dormancy,
397 and in the late summer is higher than that without dormancy, especially in the RCP 8.5 scenario.
398 The combined flattening patterns of NPP and R_H result in different patterns for NEP. Under the
399 RCP 2.6 scenario, MIC-TEM-dormancy predicts higher NEP from June to October, but lower
400 NEP from January to April compared to MIC-TEM (Figure 10). Under the RCP 8.5 scenario,
401 MIC-TEM-dormancy predicts higher NEP from June to September, but much lower NEP in other
402 months than MIC-TEM (Figure 10).
403

404 **3.4 Regional uncertainty considering equifinality effects during 20th and 21st centuries**

405 The ensemble simulations for the 20th century is shown in Figure 11. Given the
406 uncertainty in parameters, MIC-TEM-dormancy predicts that the regional cumulative carbon
407 ranges from a carbon loss of 28.2 Pg to a carbon sink of 362.1 Pg by different ensemble
408 members, with a mean of 71.2±54.8 Pg (Figure 11). For the 21st century, MIC-TEM-dormancy
409 predicts that the region acts from a carbon source of 49.3 Pg C to a carbon sink of 296.5 Pg C,
410 with a mean of 112.7±116.5 Pg under the RCP 2.6 scenario (Figure 12). Under the RCP 8.5
411 scenario, MIC-TEM-dormancy predicts that the region acts from a carbon source of 27.1 Pg C to
412 a carbon sink of 401.3 Pg C, with a mean of 143.1±162.5 Pg (Figure 12).
413

4. Discussion

Our regional simulations with two contrasting models (MIC-TEM, MIC-TEM-dormancy) indicate the regional natural terrestrial ecosystems acted as a carbon sink in past decades, which is consistent with results from other process-based models (White et al., 2000; Houghton et al., 2007; McGuire et al., 2009; Schimel, 2013). However, the magnitudes of this sink are quite different in two models. Moreover, MIC-TEM-dormancy predicts the sink will decrease under both RCP 8.5 and RCP 2.6 scenarios during the 21st century, while MIC-TEM projects that the sink will increase under the RCP 8.5 but change to carbon source under the RCP 2.6 scenario. Estimations based on models without dormancy could fit observations of R_H as well as estimations with dormancy, but at the cost of underestimating microbial biomass (Wang et al., 2014). Differences in predicted R_H with and without dormancy increase with temperature and with the length of the dry periods between wetting events (Salazar et al., 2018). The large difference in two models suggests the importance of incorporating microbial dormancy effects.

The large bias between dormancy and non-dormancy models mainly comes from two parts. First, many important microbial activities such as soil organic carbon decomposition and nutrient cycling largely depend on the active fraction of microbial communities, not total microbial biomass (Wang et al., 2014; Blagodatsky et al., 2000). However, only a small part (about 0.1-2%, seldom exceed 5%) of the total soil microbial biomass is recognized to be active under natural conditions (Blagodatsky et al., 2011; Werf & Verstraete, 1987). Thus, dormancy could be a prominent feature in soil systems (Wang et al., 2014). Without considering dormancy, the "effective" microbial biomass for soil decomposition could be overestimated, resulting in overestimation of heterotrophic respiration (He et al., 2015). He et al. (2015) predicted total soil R_H of all temperate forests (25°N-50°N) from the dormancy model amounted to 7.28 Pg C yr^{-1}

437 and 8.83 Pg C yr^{-1} from a no-dormancy model, which is 21.3% higher than the dormancy model.
438 Although their study region and simulation period are different from our study, the results can
439 still be comparable. Both studies indicated that the magnitude of R_H from no-dormancy model
440 are higher than dormancy models. Second, high soil respiration stimulates N mineralization in
441 soils (Zhuang et al., 2001, 2002), making more nutrients for photosynthesis of plants (Raich et
442 al., 1991; McGuire et al., 1995; Zhuang et al., 2015; Zha & Zhuang, 2018; Thullner et al., 2005).
443 Therefore, NPP will be higher due to the N enrichment from higher R_H. However, how NEP
444 will change is still unclear. Our estimates of the northern extratropical NEP in the 1980s (1.61 Pg
445 C yr^{-1} with MIC-TEM-dormancy and 0.84 Pg C yr^{-1} with MIC-TEM) are within ranges (0.6 to
446 2.3 PgC yr^{-1}) reported in the literature for northern regions (Schimel et al.,2001). Moreover, our
447 predicted time trajectory of NEP in the 21st century under the RCP 2.6 scenario is very similar to
448 the finding of White et al. (2000), indicating that NEP increases from the 2000s to the 2070s, and
449 then decreases in the 2090s. Although our dormancy model can project reasonable carbon fluxes
450 and indicate the importance of incorporating microbial dormancy when compared with MIC-
451 TEM (Zha & Zhuang et al., 2018), there are some other microbial traits have not yet been
452 considered in our model. For instance, one vital common evolutionary trait of microbe is the
453 community shift (Wang et al., 2015) with changing environment, including warming, N
454 fertilization and precipitation (Treseder et al., 2011; Frey et al., 2013; Allison et al., 2009; Evans
455 & Wallenstein, 2011). Community shift will influence microbial physiology, temperature
456 sensitivity and growth rates (Classen et al., 2015), which will further affect the rate of soil
457 decomposition and other carbon dynamics (Treseder et al., 2011; Schimel & Schaeffer, 2012;
458 Todd-Brown et al., 2011). Besides, microbial community composition was ignored in our model.
459 We didn't separate among functional microbial groups, but gather microbes into one "box".

However, microbial community composition could influence ecosystem functioning, and their variance in responses to environmental conditions could alter the prediction of the rates of decomposition of organic material (Balser et al. 2002; Fierer et al. 2007). Especially, some narrowly-distributed functions can be more sensitive to microbial community composition, and these might benefit most from explicit consideration of distinguishing functional groups in ecosystem models (McGuire & Treseder, 2010; Schimel 1995). Thus, functional dissimilarity in microbial communities can be considered in next step for model development (Strickland et al., 2009; Moorhead et al., 2006). Moreover, microbial acclimation, a mechanism of adaption to a new temperature regime, is another important trait to affect soil decomposition. Recent studies have found that the warming-induced elevated respiration of the microbial community could decrease over time because of acclimation (Melillo et al. 1993; Todd-Brown et al., 2011). This mechanism shall be factored into future soil decomposition analysis.

Except for model limitations mentioned above, additional uncertainties may come from inadequate model parameterization and model assumptions. For example, a critical microbial parameter, carbon use efficiency (CUE), is a primary control to soil CO_2 efflux. Higher CUE indicates more microbial growth and more carbon uptake by plants, while lower CUE indicates higher soil decomposition (Manzoni et al., 2012). Theoretical and empirical studies have suggested that CUE depends on both temperature and substrate quality (Frey et al., 2013) and decreases as temperature increases and nutrient availability decreases (Manzoni et al., 2012). Our study considered the CUE sensitivity to temperature, but not nutrient availability. On the other hand, some model assumptions can also cause uncertainties. For example, we assumed that vegetation will not change during the transient simulation. However, over the past few decades in northern temperate and boreal regions, temperature increases have led to vegetation shift from

one type to another (Hansen et al., 2006; White et al., 2000). The vegetation changes will affect carbon cycling in these ecosystems.

While our analysis suggests it is important to incorporate microbial dormancy dynamics into a process-based biogeochemistry model to more adequately simulate carbon dynamics in northern temperate and boreal regions, we do confront modeling dilemmas. First, our process-based models have a relatively large number of parameters, which unavoidably creates the "equifinality" problem as recognized in our previous studies for the model (e.g., Tang and Zhuang, 2008, 2009). To alleviate this problem in this analysis, we have conducted parameter ensemble simulations at both site and regional levels and presented our results with uncertainties, which could be a standard approach for process-based complex biogeochemistry modeling analyses. Second, incorporating more ecosystem processes increases the number of parameters in our model, inducing even larger uncertainties for both site level and regional simulations. On the one hand, the more complex model to a certain degree helps capture observations, on the other hand, the model uncertainty has not been constrained or even enlarged. We highlight the need to further investigate this trade-off within the modeling research community.

5. Conclusions

This study incorporated microbial dormancy into a detailed microbial-based soil decomposition biogeochemistry model to examine the fate of large soil carbon storage in northern temperate and boreal natural terrestrial ecosystems under changing climate conditions. Regional simulations using MIC-TEM-dormancy indicated that, over the 20th century, the region is a carbon sink of 166.8 ± 97.7 Pg. This sink could decrease to 175.9 ± 105.4 Pg under the RCP 8.5 scenario or 125.4 ± 85.5 Pg under the RCP 2.6 scenario during the 21st century. Whether

506 considering microbial dormancy or not can cause large differences in soil decomposition
507 estimation between two models. Meanwhile, due to available nitrogen affected by soil
508 decomposition, net primary production is consequently influenced in these two centuries. The
509 combined changes in soil decomposition and net primary production led to large differences in
510 carbon budget estimation between two models. Compared with MIC-TEM, MIC-TEM-
511 dormancy projected 75.9 Pg more C stored in the terrestrial ecosystems over the last century,
512 50.4 Pg and 125.2 Pg more C under the RCP 8.5 and RCP 2.6 scenarios, respectively. This study
513 highlights the importance of the representation of microbial dormancy in earth system models in
514 order to adequately quantify the carbon dynamics of natural terrestrial ecosystems in northern
515 temperate and boreal regions.
516

517 **Acknowledgments**

518 This research was supported by a NSF project (IIS-1027955), a DOE project (DE-SC0008092),
519 and a NASA LCLUC project (NNX09AI26G) to Q. Z. We acknowledge the Rosen High
520 Performance Computing Center at Purdue for computing support. We thank the National Snow
521 and Ice Data center for providing Global Monthly EASE-Grid Snow Water Equivalent data,
522 National Oceanic and Atmospheric Administration for North American Regional Reanalysis
523 (NARR). We also acknowledge the World Climate Research Programme's Working Group on
524 Coupled Modeling Intercomparison Project CMIP5, and we thank the climate modeling groups
525 for producing and making available their model output. The data presented in this paper can be
526 accessed through our research website (http://www.eaps.purdue.edu/ebdl/)

527
528
529
530

References:

Allison, E. H., Perry, A. L., Badjeck, M.-C., Neil Adger, W., Brown, K., Conway, D., Halls, A. S., Pilling, G. M., Reynolds, J. D., Andrew, N. L., and Dulvy, N. K.: Vulnerability of national economies to the impacts of climate change on fisheries, Fish and Fisheries, 10, 173-196, 10.1111/j.1467-2979.2008.00310.x, 2009.

Allison, S. D., Wallenstein, M. D., and Bradford, M. A.: Soil-carbon response to warming dependent on microbial physiology, Nature Geoscience, 3, 336-340, 10.1038/ngeo846, 2010.

Balser, T. C., Kinzig, A. P., and Firestone, M. K.: Linking soil microbial communities and ecosystem functioning, The functional consequences of biodiversity: Empirical progress and theoretical extensions, 265-293, 2002.

Blagodatskaya, E., and Kuzyakov, Y.: Active microorganisms in soil: Critical review of estimation criteria and approaches, Soil Biology and Biochemistry, 67, 192-211, 10.1016/j.soilbio.2013.08.024, 2013.

Blagodatskaya, E., Khomyakov, N., Myachina, O., Bogomolova, I., Blagodatsky, S., and Kuzyakov, Y.: Microbial interactions affect sources of priming induced by cellulose, Soil Biology and Biochemistry, 74, 39-49, 10.1016/j.soilbio.2014.02.017, 2014.

Blagodatsky, S., Grote, R., Kiese, R., Werner, C., and Butterbach-Bahl, K.: Modelling of microbial carbon and nitrogen turnover in soil with special emphasis on N-trace gases emission, Plant and soil, 346, 297-330, 10.1007/s11104-011-0821-z, 2011.

Blagodatsky, S. A., Heinemeyer, O., and Richter, J.: Estimating the active and total soil microbial biomass by kinetic respiration analysis, Biol Fertil Soils, 32, 73-81, 2000.

Bond-Lamberty, B., and Thomson, A.: Temperature-associated increases in the global soil respiration record, Nature, 464, 579-582, 10.1038/nature08930, 2010.

Bond-Lamberty, B., Bailey, V. L., Chen, M., Gough, C. M., and Vargas, R.: Globally rising soil heterotrophic respiration over recent decades, Nature, 560, 80-83, 10.1038/s41586-018-0358-x, 2018.

Bouskill, N. J., Tang, J., Riley, W. J., and Brodie, E. L.: Trait-based representation of biological nitrification: model development, testing, and predicted community composition, Frontiers in microbiology, 3, 364, 10.3389/fmicb.2012.00364, 2012.

Callaghan, T., Björn, L. O., Chernov, Y., Chapin, T., Christensen, T. R., Huntley, B., Ims, R., Jolly, D., Jonasson, S., Matveyeva, N., Panikov, N., Oechel, W., and Shaver, G.: Arctic tundra and polar desert ecosystems, Arctic climate impact assessment, 243-352, 2005.

Carney, K. M., and Matson, P. A.: The influence of tropical plant diversity and composition on soil microbial communities, Microbial ecology, 52, 226-238, 10.1007/s00248-006-9115-z, 2006.

Chmlelewrki, R. A. N., and Frank, J. F.: Formation of viable but nonculturable Salmonella during starvation in chemically defined solutions, Letters in Applied Microbiology, 20, 380-384, 1995.

Classen, A. T., Sundqvist, M. K., Henning, J. A., Newman, G. S., Moore, J. A. M., Cregger, M. A., Moorhead, L. C., and Patterson, C. M.: Direct and indirect effects of climate change on soil microbial and soil microbial-plant interactions: What lies ahead?, Ecosphere, 6, art130, 10.1890/es15-00217.1, 2015.

Conant, R. T., Ryan, M. G., Ågren, G. I., Birge, H. E., Davidson, E. A., Eliasson, P. E., Evans, S. E., Frey, S. D., Giardina, C. P., Hopkins, F. M., Hyvönen, R., Kirschbaum, M. U. F., Lavallee, J. M., Leifeld, J., Parton, W. J., Megan Steinweg, J., Wallenstein, M. D., Martin Wetterstedt, J. Å., and Bradford, M. A.: Temperature and soil organic matter decomposition rates - synthesis of

current knowledge and a way forward, Global change biology, 17, 3392-3404, 10.1111/j.1365-2486.2011.02496.x, 2011.
Coursolle, C., Margolis, H. A., Barr, A. G., Black, T. A., Amiro, B. D., McCaughey, J. H., Flanagan, L. B., Lafleur, P. M., Roulet, N. T., Bourque, C. P. A., Arain, M. A., Wofsy, S. C., Dunn, A., Morgenstern, K., Orchansky, A. L., Bernier, P. Y., Chen, J. M., Kidston, J., Saigusa, N., and Hedstrom, N.: Late-summer carbon fluxes from Canadian forests and peatlands along an east–west continental transect, Canadian Journal of Forest Research, 36, 783-800, 10.1139/x05-270, 2006.
Davidson, E. A., Trumbore, S. E., and Amundson, R.: Biogeochemistry: soil warming and organic carbon content, Nature, 408, 2000.
Davidson, E. A., and Janssens, I. A.: Temperature sensitivity of soil carbon decomposition and feedbacks to climate change, Nature, 440, 165-173, 10.1038/nature04514, 2006.
Davidson, E. A., Janssens, I. A., and Luo, Y.: On the variability of respiration in terrestrial ecosystems: moving beyond Q10, Global change biology, 12, 154-164, 10.1111/j.1365-2486.2005.01065.x, 2006.
Davidson, E. A., Samanta, S., Caramori, S. S., and Savage, K.: The Dual Arrhenius and Michaelis-Menten kinetics model for decomposition of soil organic matter at hourly to seasonal time scales, Global change biology, 18, 371-384, 10.1111/j.1365-2486.2011.02546.x, 2012.
Duan, Q., Sorooshian, S., and Gupta, V. K.: Optimal use of the SCE-UA global optimization method for calibrating watershed models, Journal of Hydrology, 158, 265-284, 1994.
Evans, S. E., and Wallenstein, M. D.: Soil microbial community response to drying and rewetting stress: does historical precipitation regime matter?, Biogeochemistry, 109, 101-116, 10.1007/s10533-011-9638-3, 2011.
Fierer, N., Morse, J. L., Berthrong, S. T., Bernhardt, E. S., and Jackson, R. B.: Environmental controls on the landscape - scale biogeography of stream bacterial communities, Ecology, 88, 2162-2173, 2007.
Frey, S. D., Lee, J., Melillo, J. M., and Six, J.: The temperature response of soil microbial efficiency and its feedback to climate, Nature Climate Change, 3, 395-398, 10.1038/nclimate1796, 2013.
German, D. P., Marcelo, K. R. B., Stone, M. M., and Allison, S. D.: The Michaelis-Menten kinetics of soil extracellular enzymes in response to temperature: a cross-latitudinal study, Global change biology, 18, 1468-1479, 10.1111/j.1365-2486.2011.02615.x, 2012.
Gilmanov, T. G., Tieszen, L. L., Wylie, B. K., Flanagan, L. B., Frank, A. B., Haferkamp, M. R., Meyers, T. P., and Morgan, J. A.: Integration of CO2flux and remotely-sensed data for primary production and ecosystem respiration analyses in the Northern Great Plains: potential for quantitative spatial extrapolation, Global Ecology and Biogeography, 14, 271-292, 10.1111/j.1466-822X.2005.00151.x, 2005.
Gough, C. M., Hardiman, B. S., Nave, L. E., Bohrer, G., Maurer, K. D., Vogel, C. S., Nadelhoffer, K. J., and Curtis, P. S.: Sustained carbon uptake and storage following moderate disturbancein a Great Lakes forest, Ecological Applications, 23, 1202-1215, 2013.
Goulden, M. L., Winston, G. C., McMillan, A. M. S., Litvak, M. E., Read, E. L., Rocha, A. V., and Rob Elliot, J.: An eddy covariance mesonet to measure the effect of forest age on land?atmosphere exchange, Global change biology, 12, 2146-2162, 10.1111/j.1365-2486.2006.01251.x, 2006.
Graham, E. B., Wieder, W. R., Leff, J. W., Weintraub, S. R., Townsend, A. R., Cleveland, C. C., Philippot, L., and Nemergut, D. R.: Do we need to understand microbial communities to predict

ecosystem function? A comparison of statistical models of nitrogen cycling processes, Soil Biology and Biochemistry, 68, 279-282, 10.1016/j.soilbio.2013.08.023, 2014.
Graham, E. B., Knelman, J. E., Schindlbacher, A., Siciliano, S., Breulmann, M., Yannarell, A., Beman, J. M., Abell, G., Philippot, L., Prosser, J., Foulquier, A., Yuste, J. C., Glanville, H. C., Jones, D. L., Angel, R., Salminen, J., Newton, R. J., Burgmann, H., Ingram, L. J., Hamer, U., Siljanen, H. M., Peltoniemi, K., Potthast, K., Baneras, L., Hartmann, M., Banerjee, S., Yu, R. Q., Nogaro, G., Richter, A., Koranda, M., Castle, S. C., Goberna, M., Song, B., Chatterjee, A., Nunes, O. C., Lopes, A. R., Cao, Y., Kaisermann, A., Hallin, S., Strickland, M. S., Garcia-Pausas, J., Barba, J., Kang, H., Isobe, K., Papaspyrou, S., Pastorelli, R., Lagomarsino, A., Lindstrom, E. S., Basiliko, N., and Nemergut, D. R.: Microbes as Engines of Ecosystem Function: When Does Community Structure Enhance Predictions of Ecosystem Processes?, Frontiers in microbiology, 7, 214, 10.3389/fmicb.2016.00214, 2016.
Griffis, T. J., Lee, X., Baker, J. M., Billmark, K., Schultz, N., Erickson, M., Zhang, X., Fassbinder, J., Xiao, W., and Hu, N.: Oxygen isotope composition of evapotranspiration and its relation to C4photosynthetic discrimination, Journal of Geophysical Research, 116, 10.1029/2010jg001514, 2011.
Hagerty, S. B., van Groenigen, K. J., Allison, S. D., Hungate, B. A., Schwartz, E., Koch, G. W., Kolka, R. K., and Dijkstra, P.: Accelerated microbial turnover but constant growth efficiency with warming in soil, Nature Climate Change, 4, 903-906, 10.1038/nclimate2361, 2014.
Hansen, J., Sato, M., Ruedy, R., Lo, K., Lea, D. W., and Medina-Elizade, M.: Global temperature change, Proceedings of the National Academy of Sciences of the United States of America, 103, 14288-14293, 10.1073/pnas.0606291103, 2006.
Harder, w., and Dijkhuizen, L.: Physiological responses to nutrient limitation, Annual Review of Microbiology, 37, 1983.
Harris, I., Jones, P. D., Osborn, T. J., and Lister, D. H.: Updated high-resolution grids of monthly climatic observations - the CRU TS3.10 Dataset, International Journal of Climatology, 34, 623-642, 10.1002/joc.3711, 2014.
He, Y., Yang, J., Zhuang, Q., Harden, J. W., McGuire, A. D., Liu, Y., Wang, G., and Gu, L.: Incorporating microbial dormancy dynamics into soil decomposition models to improve quantification of soil carbon dynamics of northern temperate forests, Journal of Geophysical Research: Biogeosciences, 120, 2596-2611, 10.1002/2015jg003130, 2015.
Hiller, R. V., McFadden, J. P., and Kljun, N.: Interpreting CO2 Fluxes Over a Suburban Lawn: The Influence of Traffic Emissions, Boundary-Layer Meteorology, 138, 215-230, 10.1007/s10546-010-9558-0, 2010.
Houghton, R. A.: Balancing the Global Carbon Budget, Annual Review of Earth and Planetary Sciences, 35, 313-347, 10.1146/annurev.earth.35.031306.140057, 2007.
Hugelius, G., Strauss, J., Zubrzycki, S., Harden, J. W., Schuur, E. A. G., Ping, C. L., Schirrmeister, L., Grosse, G., Michaelson, G. J., Koven, C. D., amp, apos, Donnell, J. A., Elberling, B., Mishra, U., Camill, P., Yu, Z., Palmtag, J., and Kuhry, P.: Estimated stocks of circumpolar permafrost carbon with quantified uncertainty ranges and identified data gaps, Biogeosciences, 11, 6573-6593, 10.5194/bg-11-6573-2014, 2014.
Jenkins, J. P., Richardson, A. D., Braswell, B. H., Ollinger, S. V., Hollinger, D. Y., and Smith, M. L.: Refining light-use efficiency calculations for a deciduous forest canopy using simultaneous tower-based carbon flux and radiometric measurements, Agricultural and Forest Meteorology, 143, 64-79, 10.1016/j.agrformet.2006.11.008, 2007.

667 Kaiser, C., Franklin, O., Dieckmann, U., and Richter, A.: Microbial community dynamics
668 alleviate stoichiometric constraints during litter decay, Ecology letters, 17, 680-690,
669 10.1111/ele.12269, 2014.
670 Knorr, W., Prentice, I. C., House, J. I., and Holland, E. A.: Long-term sensitivity of soil carbon
671 turnover to warming, Nature, 433, 2005.
672 Lawrence, C. R., Neff, J. C., and Schimel, J. P.: Does adding microbial mechanisms of
673 decomposition improve soil organic matter models? A comparison of four models using data
674 from a pulsed rewetting experiment, Soil Biology and Biochemistry, 41, 1923-1934,
675 10.1016/j.soilbio.2009.06.016, 2009.
676 Lennon, J. T., and Jones, S. E.: Microbial seed banks: the ecological and evolutionary
677 implications of dormancy, Nature reviews. Microbiology, 9, 119-130, 10.1038/nrmicro2504,
678 2011.
679 Lloyd, A. H., Rupp, T. S., Fastie, C. L., and Starfield, A. M.: Patterns and dynamics of treeline
680 advance on the Seward Peninsula, Alaska, Journal of Geophysical Research, 108,
681 10.1029/2001jd000852, 2002.
682 Manzoni, S., Taylor, P., Richter, A., Porporato, A., and Agren, G. I.: Environmental and
683 stoichiometric controls on microbial carbon-use efficiency in soils, The New phytologist, 196,
684 79-91, 10.1111/j.1469-8137.2012.04225.x, 2012.
685 McEwing, K. R., Fisher, J. P., and Zona, D.: Environmental and vegetation controls on the
686 spatial variability of CH4 emission from wet-sedge and tussock tundra ecosystems in the Arctic,
687 Plant and soil, 388, 37-52, 10.1007/s11104-014-2377-1, 2015.
688 McGuire, A. D., Melillo, J. M., Joyce, L. A., Kicklighter, D. W., Grace, A. L., III, B. M., and
689 Vorosmarty, C. J.: Interactions between carbon and nitrogen dynamics in estimating net primary
690 productivity for potential vegetation in North America, Global Biogeochemical Cycles, 6, 101-
691 124, 1992.
692 McGuire, A. D., Melillo, J. M., Kicklighter, D. W., and Joyce, L. A.: Equilibrium responses of
693 soil carbon to climate change: Empirical and process-based estimates, Journal of Biogeography,
694 22, 785-796, 1995.
695 McGuire, A. D., and Hobbie, J. E.: Global climate change and the equilibrium responses of
696 carbon storage in arctic and subarctic regions, In Modeling the Arctic system: A workshop report
697 on the state of modeling in the Arctic System Science program, 53-54, 1997.
698 McGuire, A. D., Anderson, L. G., Christensen, T. R., Dallimore, S., Guo, L., Hayes, D. J.,
699 Heimann, M., Lorenson, T. D., Macdonald, R. W., and Roulet, N.: Sensitivity of the carbon
700 cycle in the Arctic to climate change, Ecological Monographs, 79, 523-555, 2009.
701 McGuire, K. L., and Treseder, K. K.: Microbial communities and their relevance for ecosystem
702 models: Decomposition as a case study, Soil Biology and Biochemistry, 42, 529-535,
703 10.1016/j.soilbio.2009.11.016, 2010.
704 Me´tris, A., Gerrard, A. M., Cumming, R. H., Weigner, P., and Paca, J.: Modelling shock
705 loadings and starvation in the biofiltration of toluene and xylene, Journal of Chemical
706 Technology and Biotechnology, 76, 565-572, 2001.
707 Melillo, J. M., McGuire, A. D., Kicklighter, D. W., III, B. M., Vorosmarty, C. J., and Schloss, A.
708 L.: Global climate change and terrestrial net primary production, Nature, 363, 1993.
709 Merbold, L., Kutsch, W. L., Corradi, C., Kolle, O., Rebmann, C., Stoy, P. C., Zimov, S. A., and
710 Schulze, E. D.: Artificial drainage and associated carbon fluxes (CO2/CH4) in a tundra
711 ecosystem, Global change biology, 15, 2599-2614, 10.1111/j.1365-2486.2009.01962.x, 2009.

712 Moorhead, D. L., and Sinsabaugh, R. L.: A theoretical model of litter decay and microbial
713 interaction, Ecological Monographs, 76, 151-174, 2006.
714 Oechel, W. C., Laskowski, C. A., Burba, G., Gioli, B., and Kalhori, A. A. M.: Annual patterns
715 and budget of CO2flux in an Arctic tussock tundra ecosystem, Journal of Geophysical Research:
716 Biogeosciences, 119, 323-339, 10.1002/2013jg002431, 2014.
717 P.J. Hanson, N. T. E., C.T. Garten, J.A. Andrews: Separating root and soil microbial
718 contributions to soil respiration: A review of methods and observations, Biogeochemistry, 48,
719 115-146, 2000.
720 Parton, W. J., Scurlock, J. M. O., Ojima, D. S., Gilmanov, T. G., Scholes, R. J., Schimel, D. S.,
721 Kirchner, T., Menaut, J. C., Seastedt, T., Moya, E. G., Kamnalrut, A., and Kinyamario, J. I.:
722 Observations and modeling of biomass and soil organic matter dynamics for the grassland biome
723 worldwide, Global Biogeochemical Cycles, 7, 785-809, 1993.
724 Raich, J. W., Rastetter, E. B., Melillo, J. M., Kicklighter, D. W., Steudler, P. A., Peterson, B. J.,
725 Grace, A. L., III, B. M., and Vorosmarty, C. J.: Potential net primary productivity in South
726 America: application of a global model, Ecological Applications, 1, 399-429, 1991.
727 Richardson, A. D., Jenkins, J. P., Braswell, B. H., Hollinger, D. Y., Ollinger, S. V., and Smith,
728 M. L.: Use of digital webcam images to track spring green-up in a deciduous broadleaf forest,
729 Oecologia, 152, 323-334, 10.1007/s00442-006-0657-z, 2007.
730 Running, S. W., and Coughlan, J. C.: A general model of forest ecosystem processes for regional
731 applications I. Hydrologic balance, canopy gas exchange and primary production processes.,
732 Ecological Modelling, 42, 125-154, 1988.
733 Schimel, D. S.: Terrestrial ecosystems and the carbon cycle, Global change biology, 1, 77-91,
734 1995.
735 Schimel, D. S., House, J. I., Hibbard, K. A., Bousquet, P., Ciais, P., Peylin, P., Braswell, B. H.,
736 Apps, M. J., Baker, D., Bondeau, A., Canadell, J., Churkina, G., Cramer, W., Denning, A. S.,
737 Field, C. B., Friedlingstein, P., Goodale, C., Heimann, M., Houghton, R. A., Melillo, J. M., III,
738 B. M., Murdiyarso, D., Noble, I., Pacala, S. W., Prentice, I. C., Raupach, M. R., Rayner, P. J.,
739 Scholes, R. J., Steffen, W. L., and Wirth, C.: Recent patterns and mechanisms of carbon
740 exchange by terrestrial ecosystems, Nature, 414, 2001.
741 Schimel, J.: Microbes and global carbon, Nature Climate Change, 3, 867-868,
742 10.1038/nclimate2015, 2013.
743 Schimel, J. P., and Weintraub, M. N.: The implications of exoenzyme activity on microbial
744 carbon and nitrogen limitation in soil: a theoretical model, Soil Biology and Biochemistry, 35,
745 549-563, 10.1016/s0038-0717(03)00015-4, 2003.
746 Schimel, J. P., and Schaeffer, S. M.: Microbial control over carbon cycling in soil, Frontiers in
747 microbiology, 3, 348, 10.3389/fmicb.2012.00348, 2012.
748
749 Schmidt, M. W., Torn, M. S., Abiven, S., Dittmar, T., Guggenberger, G., Janssens, I. A., Kleber,
750 M., Kogel-Knabner, I., Lehmann, J., Manning, D. A., Nannipieri, P., Rasse, D. P., Weiner, S.,
751 and Trumbore, S. E.: Persistence of soil organic matter as an ecosystem property, Nature, 478,
752 49-56, 10.1038/nature10386, 2011.
753
754 Stolpovsky, K., Martinez-Lavanchy, P., Heipieper, H. J., Van Cappellen, P., and Thullner, M.:
755 Incorporating dormancy in dynamic microbial community models, Ecological Modelling, 222,
756 3092-3102, 10.1016/j.ecolmodel.2011.07.006, 2011.

Stow, D. A., Hope, A., McGuire, D., Verbyla, D., Gamon, J., Huemmrich, F., Houston, S., Racine, C., Sturm, M., Tape, K., Hinzman, L., Yoshikawa, K., Tweedie, C., Noyle, B., Silapaswan, C., Douglas, D., Griffith, B., Jia, G., Epstein, H., Walker, D., Daeschner, S., Petersen, A., Zhou, L., and Myneni, R.: Remote sensing of vegetation and land-cover change in Arctic Tundra Ecosystems, Remote Sensing of Environment, 89, 281-308, 10.1016/j.rse.2003.10.018, 2004.

Strickland, M. S., Lauber, C., Fierer, N., and Bradford, M. A.: Testing the functional significanceof microbial community composition, Ecology, 90, 441-451, 2009.

Tang, J., Q. Zhuang (2009) A global sensitivity analysis and Bayesian inference framework for improving the parameter estimation and prediction of a process-based Terrestrial Ecosystem Model J. Geophys. Res., 114, D15303, doi:10.1029/2009JD011724., 2009.

Tang, J., Q. Zhuang (2008) Equifinality in parameterization of process-based biogeochemistry models: A significant uncertainty source to the estimation of regional carbon dynamics J. Geophys. Res., 113, G04010, doi:10.1029/2008JG000757, 2008.

Tang, J., and Riley, W. J.: Weaker soil carbon–climate feedbacks resulting from microbial and abiotic interactions, Nature Climate Change, 5, 56-60, 10.1038/nclimate2438, 2014.

Tape, K. E. N., Sturm, M., and Racine, C.: The evidence for shrub expansion in Northern Alaska and the Pan-Arctic, Global change biology, 12, 686-702, 10.1111/j.1365-2486.2006.01128.x, 2006.

Tarnocai, C., Canadell, J. G., Schuur, E. A. G., Kuhry, P., Mazhitova, G., and Zimov, S.: Soil organic carbon pools in the northern circumpolar permafrost region, Global Biogeochemical Cycles, 23, n/a-n/a, 10.1029/2008gb003327, 2009.

Thullner, M., Van Cappellen, P., and Regnier, P.: Modeling the impact of microbial activity on redox dynamics in porous media, Geochimica et Cosmochimica Acta, 69, 5005-5019, 10.1016/j.gca.2005.04.026, 2005.

Todd-Brown, K. E. O., Hopkins, F. M., Kivlin, S. N., Talbot, J. M., and Allison, S. D.: A framework for representing microbial decomposition in coupled climate models, Biogeochemistry, 109, 19-33, 10.1007/s10533-011-9635-6, 2011.

Todd-Brown, K. E. O., Randerson, J. T., Post, W. M., Hoffman, F. M., Tarnocai, C., Schuur, E. A. G., and Allison, S. D.: Causes of variation in soil carbon simulations from CMIP5 Earth system models and comparison with observations, Biogeosciences, 10, 1717-1736, 10.5194/bg-10-1717-2013, 2013.

Treseder, K. K., Balser, T. C., Bradford, M. A., Brodie, E. L., Dubinsky, E. A., Eviner, V. T., Hofmockel, K. S., Lennon, J. T., Levine, U. Y., MacGregor, B. J., Pett-Ridge, J., and Waldrop, M. P.: Integrating microbial ecology into ecosystem models: challenges and priorities, Biogeochemistry, 109, 7-18, 10.1007/s10533-011-9636-5, 2011.

W. D. Billings, K. M. P., G. R. Shaver, A. W. Trent: Root Growth, Respiration, and Carbon Dioxide Evolution in an Arctic Tundra Soil, Arctic and Alpine Research, 9, 129-137, 10.1080/00040851.1977.12003908, 1977.

Wang, G., M. A. M., Lianhong Gu, Christopher W. Schadt: Representation of Dormant and Active Microbial Dynamics for Ecosystem Modeling, Public Library of Science, 9, 10.1371/journal.pone.0089252.g001, 2014.

Wang, G., Jagadamma, S., Mayes, M. A., Schadt, C. W., Steinweg, J. M., Gu, L., and Post, W. M.: Microbial dormancy improves development and experimental validation of ecosystem model, The ISME journal, 9, 226-237, 10.1038/ismej.2014.120, 2015.

Wang Wei, F. J., T. Oikawa: Contribution of Root and Microbial Respiration to Soil CO2 Efflux and Their Environmental Controls in a Humid Temperate Grassland of Japan, Pedosphere, 19, 31-39, 2009.
Werf, H. V. d., and Verstraete, W.: Estimation of active soil microbial biomass by mathematical analysis of respiration curves: relation to conventional estimation of total biomass, Soil Biology and Biochemistry, 19, 267-271, 1987.
White, A., Cannell, M. G. R., and Friend, A. D.: The high-latitude terrestrial carbon sink: a model analysis Global change biology, 6, 227-245, 2000.
Wieder, W. R., Bonan, G. B., and Allison, S. D.: Global soil carbon projections are improved by modelling microbial processes, Nature Climate Change, 3, 909-912, 10.1038/nclimate1951, 2013.
Xu, X., Schimel, J. P., Thornton, P. E., Song, X., Yuan, F., and Goswami, S.: Substrate and environmental controls on microbial assimilation of soil organic carbon: a framework for Earth system models, Ecology letters, 17, 547-555, 10.1111/ele.12254, 2014.
Zha, J., and Zhuang, Q.: Microbial decomposition processes and vulnerable arctic soil organic carbon in the 21st century, Biogeosciences, 15, 5621-5634, 10.5194/bg-15-5621-2018, 2018a.
Zha, J., and Zhuang, Q.: Microbial decomposition processes and vulnerable Arctic soil organic carbon in the 21st century, Biogeosciences Discussions, 1-34, 10.5194/bg-2018-241, 2018b.
Zhou, L., Tucker, C. J., Kaufmann, R. K., Slayback, D., Shabanov, N. V., and Myneni, R. B.: Variations in northern vegetation activity inferred from satellite data of vegetation index during 1981 to 1999, Journal of Geophysical Research: Atmospheres, 106, 20069-20083, 10.1029/2000jd000115, 2001.
Zhuang, Q., Romanovsky, V. E., and McGuire, A. D.: Incorporation of a permafrost model into a large-scale ecosystem model: Evaluation of temporal and spatial scaling issues in simulating soil thermal dynamics, Journal of Geophysical Research: Atmospheres, 106, 33649-33670, 10.1029/2001jd900151, 2001.
Zhuang, Q., McGuire, A. D., O'Neill, K. P., Harden, J. W., Romanovsky, V. E., and Yarie, J.: Modeling soil thermal and carbon dynamics of a fire chronosequence in interior Alaska, Journal of Geophysical Research, 108, 10.1029/2001jd001244, 2002.
Zhuang, Q., He, J., Lu, Y., Ji, L., Xiao, J., and Luo, T.: Carbon dynamics of terrestrial ecosystems on the Tibetan Plateau during the 20th century: an analysis with a process-based biogeochemical model, Global Ecology and Biogeography, 19, 649-662, 10.1111/j.1466-8238.2010.00559.x, 2010.
Zhuang, Q., Zhu, X., He, Y., Prigent, C., Melillo, J. M., David McGuire, A., Prinn, R. G., and Kicklighter, D. W.: Influence of changes in wetland inundation extent on net fluxes of carbon dioxide and methane in northern high latitudes from 1993 to 2004, Environmental Research Letters, 10, 095009, 10.1088/1748-9326/10/9/095009, 2015.
Zhuang, Q., McGuire, A. D., Melillo, J. M., Clein, J. S., Dargaville, R. J., Kicklighter, D. W., Myneni, R. B., Dong, J., Romanovsky, V. E., Harden, J., and Hobbie, J. E.: Carbon cycling in extratropical terrestrial ecosystems of the Northern Hemisphere during the 20th century: a modeling analysis of the influences of soil thermal dynamics, Tellus B: Chemical and Physical Meteorology, 55, 751-776, 10.3402/tellusb.v55i3.16368, 2016.

Author contributions. Q.Z. designed the study. J.Z. conducted model development, simulation and analysis. J.Z. and Q. Z. wrote the paper.

Competing financial interests. The submission has no competing financial interests.

Materials & Correspondence. Correspondence and material requests should be addressed to qzhuang@purdue.edu.

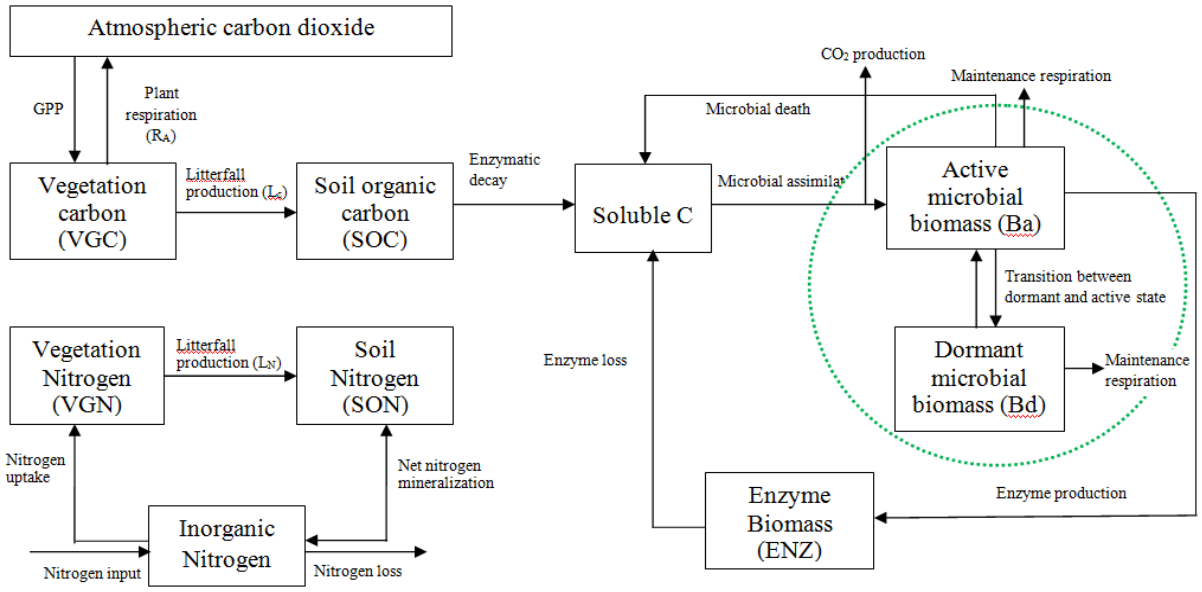

Figure 1. Framework of the dormancy model: microbial biomass is split into two parts, active microbial biomass and dormant microbial biomass (shown in the green dashed circle). Maintenance respiration from these two parts, and the CO_2 production through microbial assimilation contributes to heterotrophic respiration. The model was revised based on Zha & Zhuang (2018).

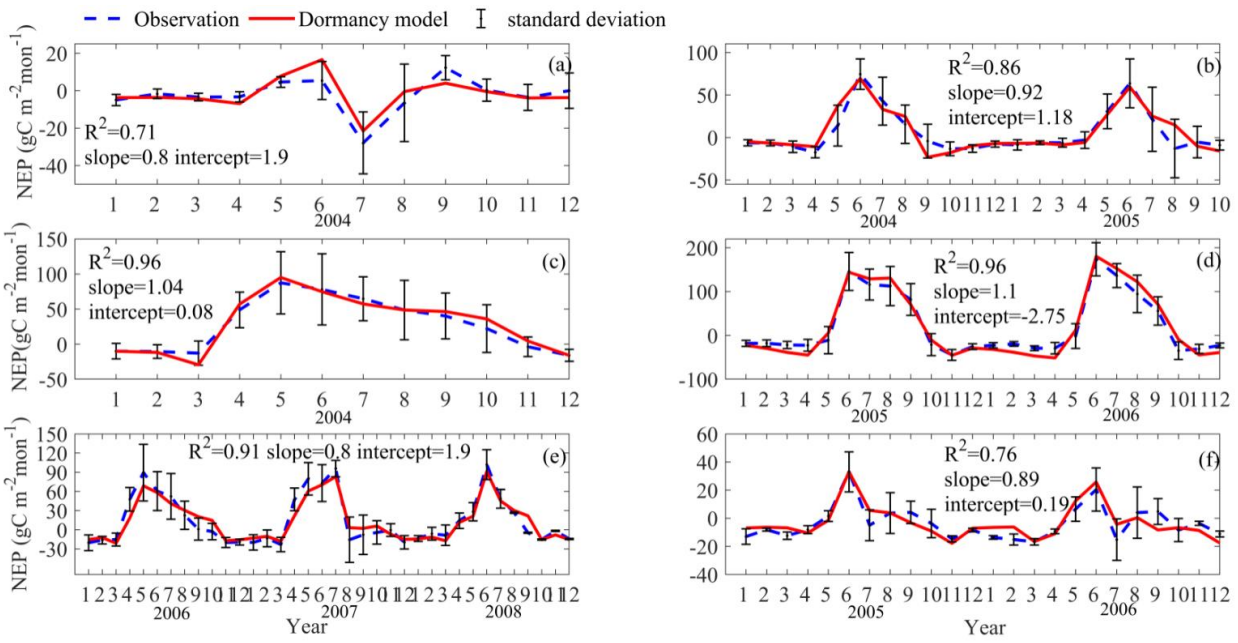

Figure 2. Comparison between observed and simulated NEP (gC $m^{-2}mon^{-1}$) at: (a) Ivotuk (alpine tundra), (b) UCI-1964 burn site (boreal forest), (c) Howland Forest (main tower) (temperate coniferous forest), (d) Univ. of Mich. Biological Station (Temperate deciduous forest), (e) KUOM Turfgrass Field (Grassland), and (f) Atqasuk (Wet tundra). Note: scales are different. Error bars represent standard errors among daily measure data in one month.

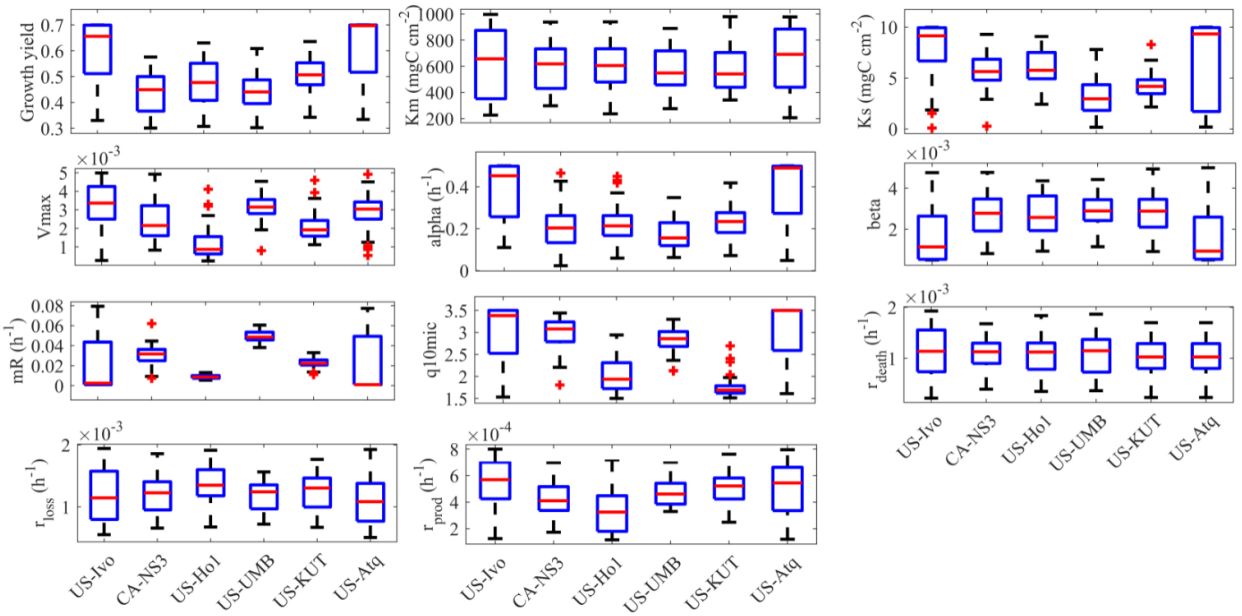

Figure 3. Boxplot of parameter posterior distribution that are obtained after ensemble inverse modeling for MIC-TEM-dormancy all six sites: US-Ivo: Ivotuk (alpine tundra), CA-NS3: UCI-1964 burn site (boreal forest), US-Ho1: Howland Forest (temperate coniferous forest), US-UMB: Univ. of Mich. Biological Station (temperate deciduous forest), US-KUT: KUOM Turfgrass Field (grassland), US-Atq: Atqasuk (wet tundra).

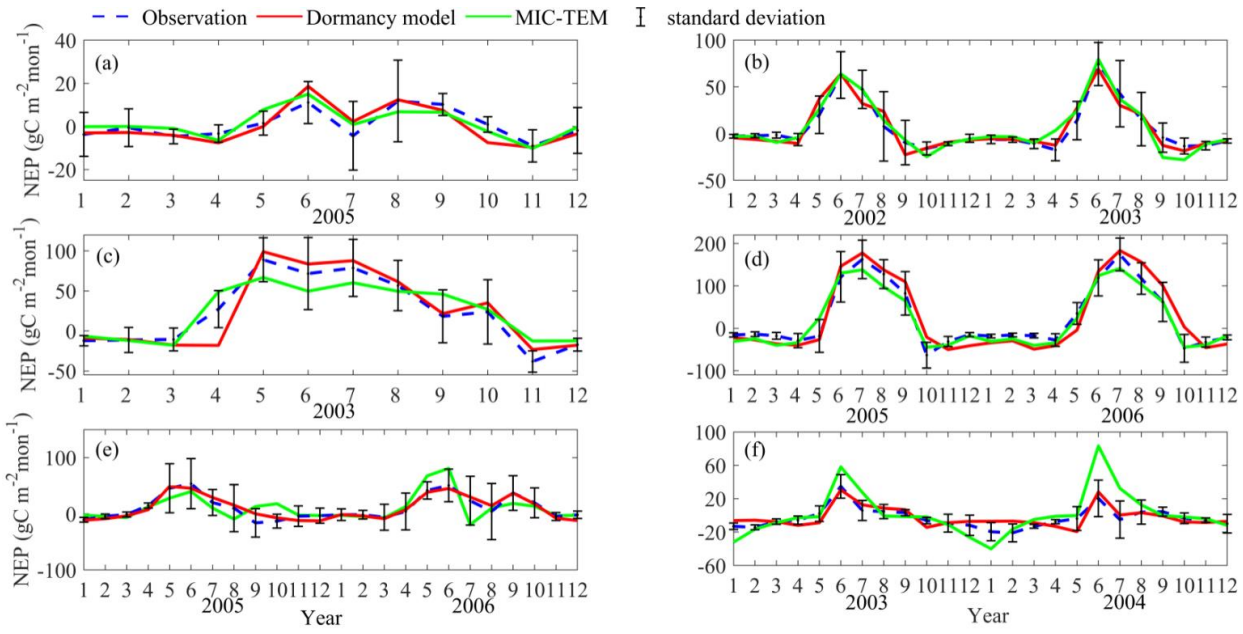

Figure 4. Comparison between observed and simulated NEP (gC $m^{-2}mon^{-1}$) at: (a) Ivotuk (alpine tundra), (b) UCI-1964 burn site (boreal forest), (c) Howland Forest (main tower) (temperate coniferous forest), (d) Bartlett Experimental Forest (Temperate deciduous forest), (e) Brookings (Grassland), and (f) Atqasuk (Wet tundra). Note: scales are different.

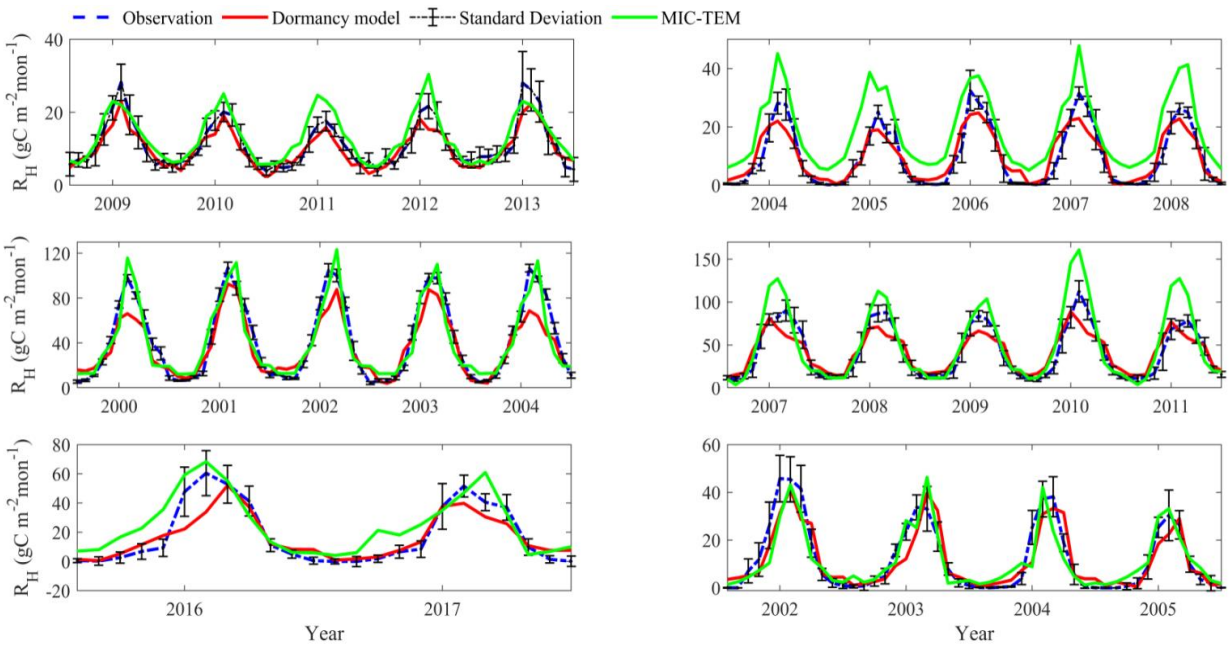

Figure 5. Comparison between observed and simulated R_H (gC $m^{-2}mon^{-1}$) at: (a) US-EML (alpine tundra), (b) CA-SJ2 (boreal forest), (c) US-Ho2 (temperate coniferous forest), (d) US-UMB (Temperate deciduous forest), (e) US-Ro4 (Grassland), and (f) RU-Che (Wet tundra). Note: scales are different.

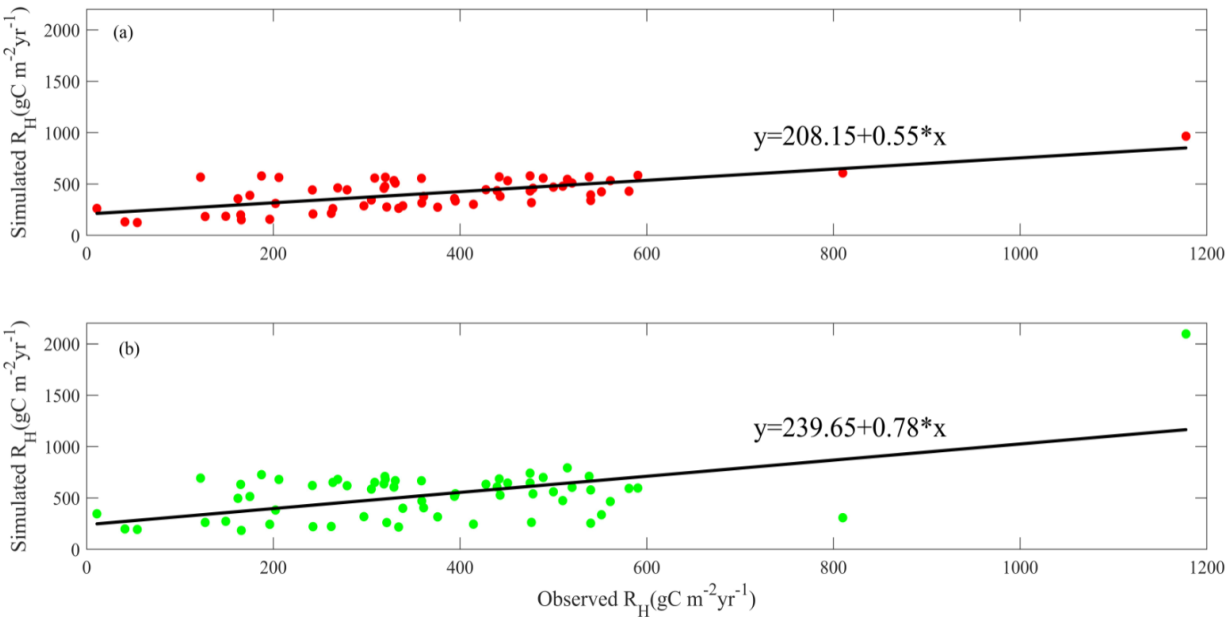

Figure 6. Linear regression between simulated and observed annual R_H (gC $m^{-2}yr^{-1}$) for: (a) MIC-TEM-dormancy, and (b) MIC-TEM.

924

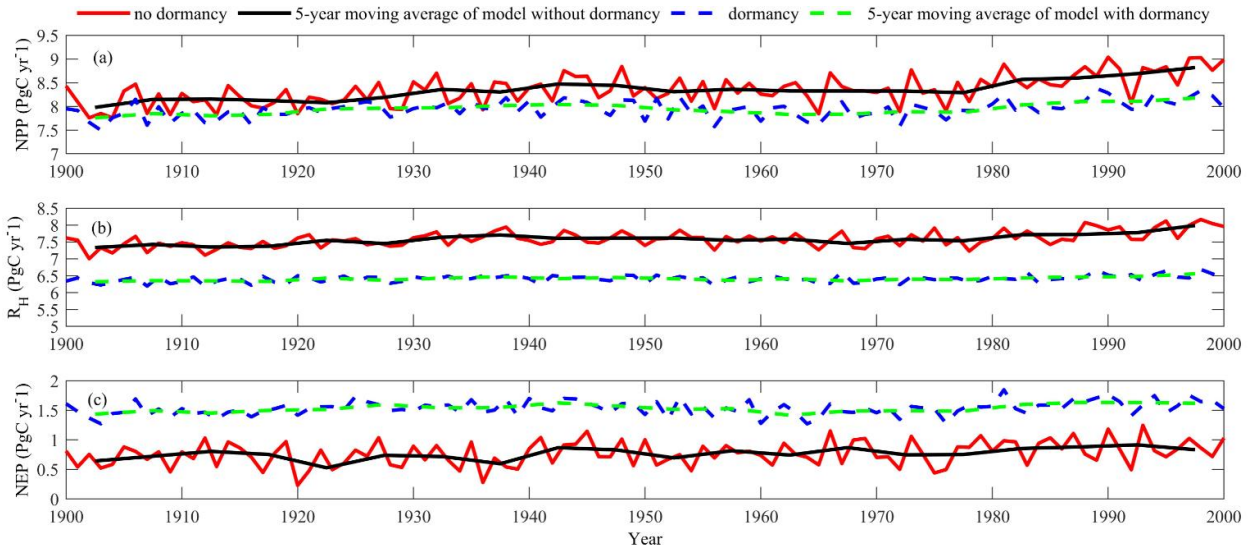

925 Figure 7. Simulated annual net primary production (NPP, top panel), heterotrophic respiration (R_H,
926 center panel) and net ecosystem production (NEP, bottom panel) during the 20th century by
927 dormancy model and MIC-TEM, respectively.

928

929

930

931

932

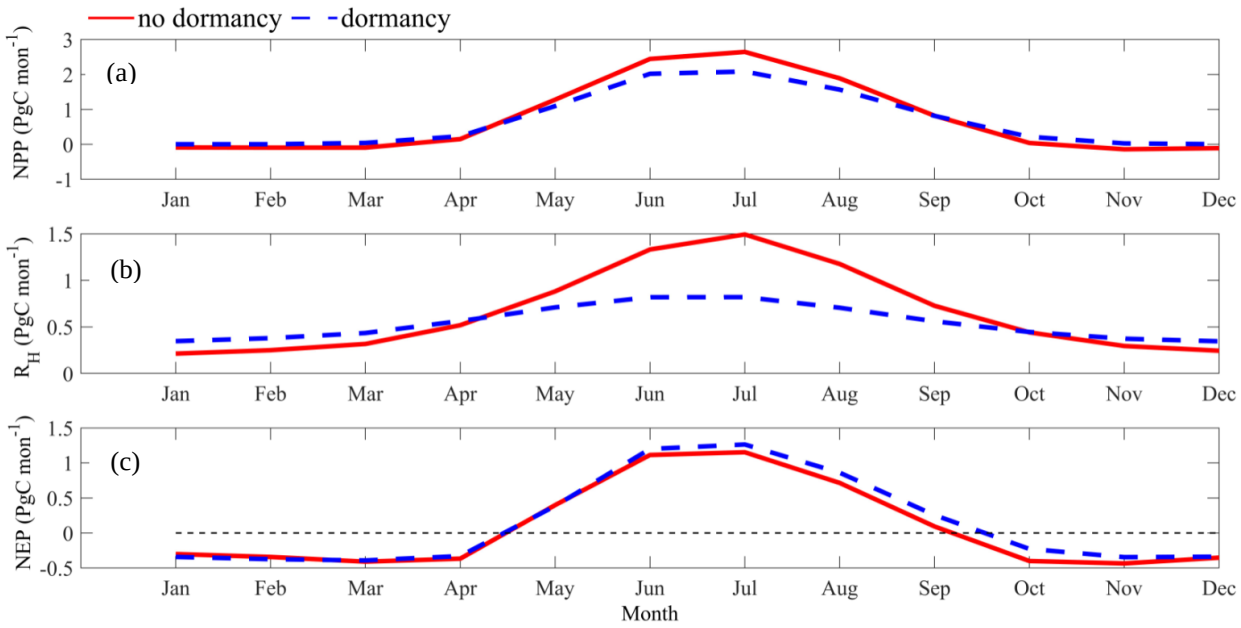

Figure 8. Regional annual seasonal pattern of simulated (a) net primary production (NPP, top panel), (b) heterotrophic respiration (R_H, center panel) and (c) net ecosystem production (NEP, bottom panel) during the 1990s from dormancy model and MIC-TEM. The region is all land areas north of 45 ºN.

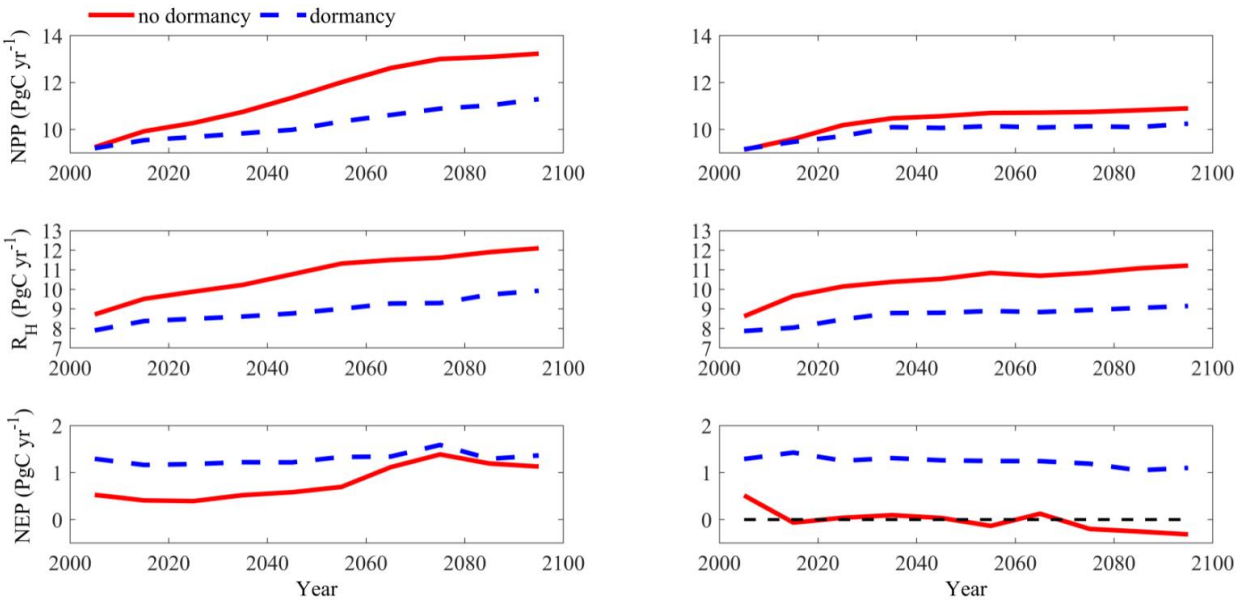

Figure 9. Predicted changes in carbon fluxes: (i) NPP, (ii) R_H, and (iii) NEP for all land areas north of 45 ºN in response to transient climate change under the RCP 8.5 scenario (left panel) and RCP 2.6 scenario (right panel) with dormancy model and MIC-TEM, respectively. The decadal running mean is applied.

(a)

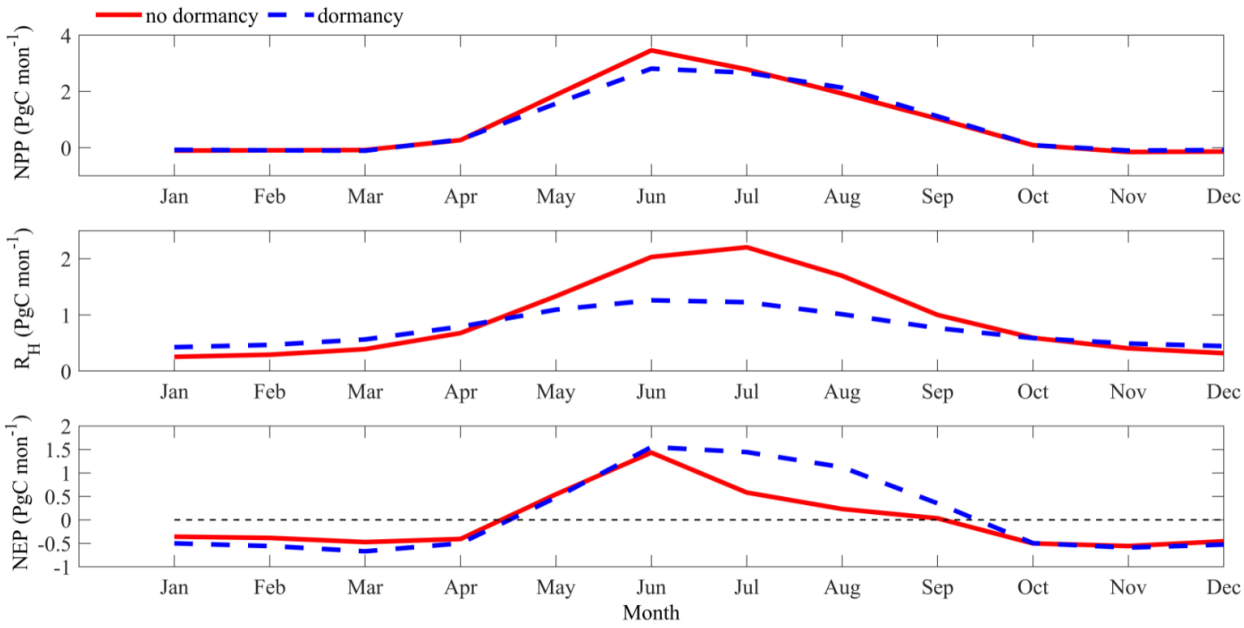

(b)

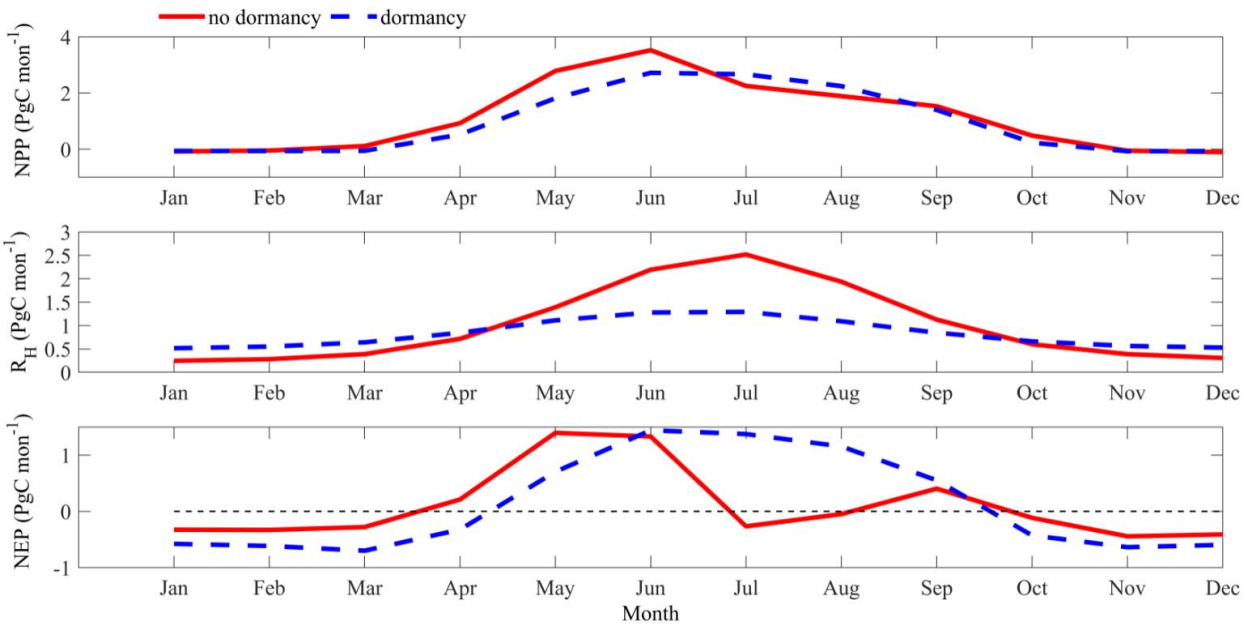

Figure 10. Regional annual seasonal pattern of simulated net primary production (NPP, top panel), heterotrophic respiration (R_H, center panel) and net ecosystem production (NEP, bottom panel) during the 2090s from dormancy model and MIC-TEM under: (a) RCP 2.6 scenario (top panel) and (b) RCP 8.5 scenario (bottom panel). The region is all land areas north of 45 ºN.

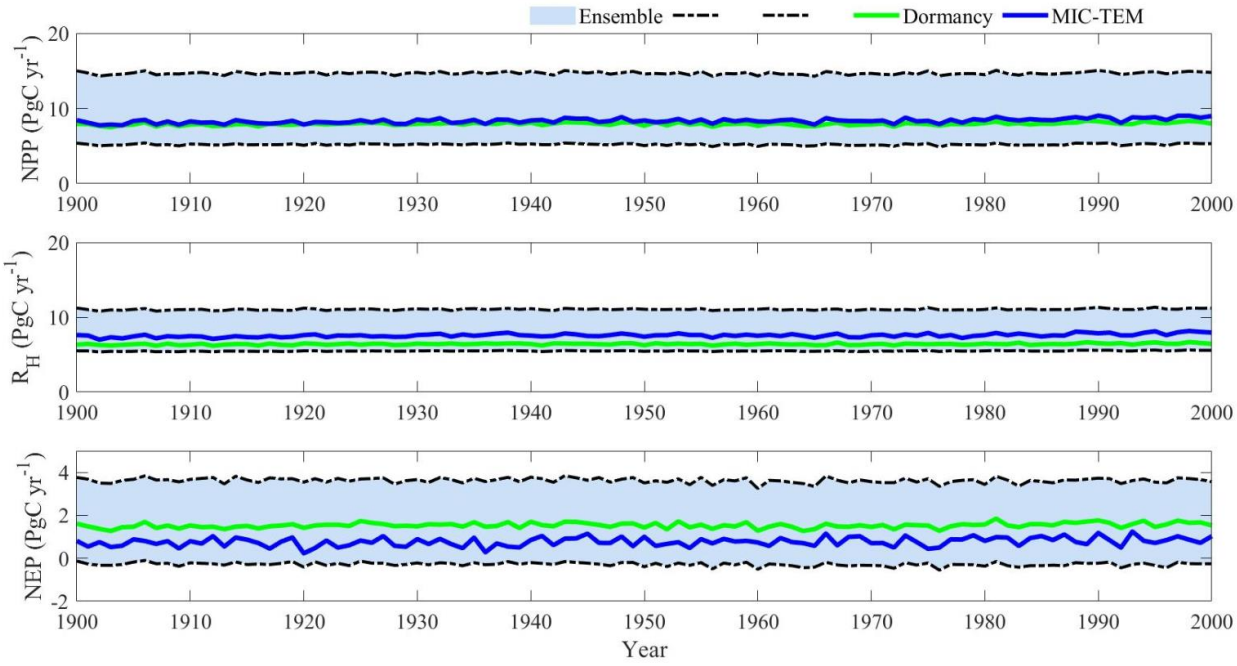

Figure 11. Simulated annual net primary production (NPP, top panel), heterotrophic respiration (R_H, center panel) and net ecosystem production (NEP, bottom panel) by MIC-TEM-dormancy with ensemble of parameters.

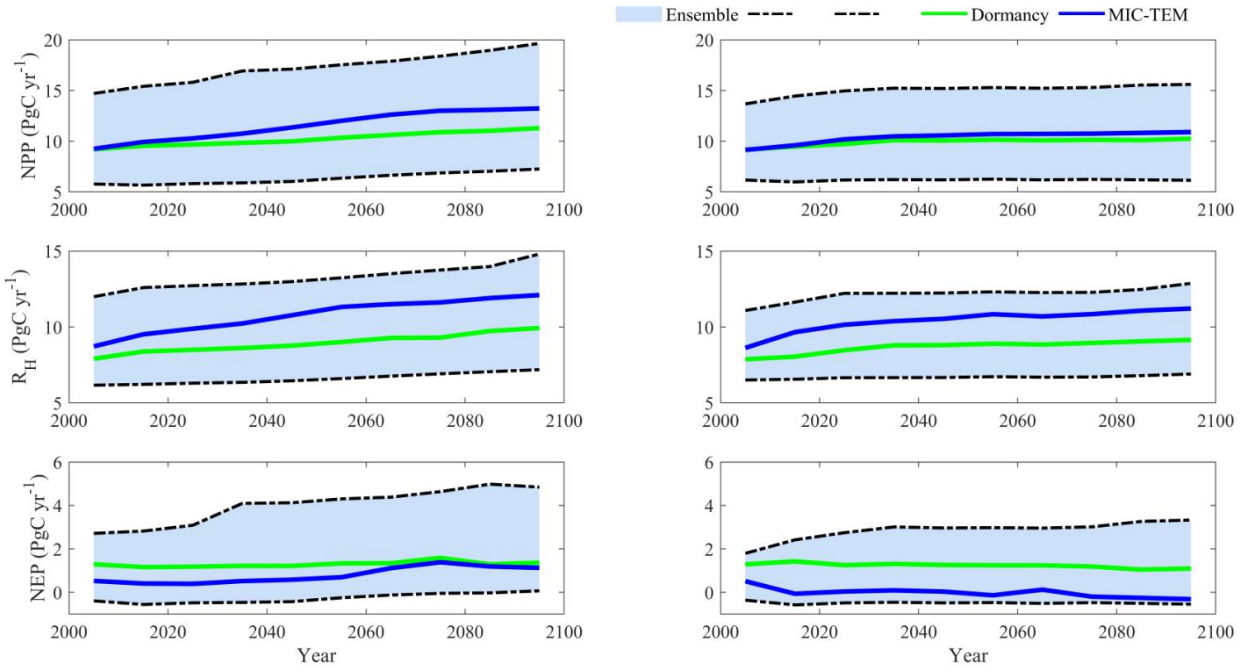

Figure 12. Simulated annual net primary production (NPP, top panel), heterotrophic respiration (R_H, center panel) and net ecosystem production (NEP, bottom panel) under RCP 8.5 scenario (left panel) and RCP 2.6 scenario (right panel) by MIC-TEM-dormancy with ensemble of parameters. The decadal running mean is applied. The grey area represents the upper and lower bounds of simulations.

Table 1. Parameters associated with detailed microbial dormancy in MIC-TEM-dormancy

parameter	unit	description	Parameter range	references
m_R	h^{-1}	Specific maintenance rate at active state	[0.001, 0.08]	Wang et al. (2014)
Q_{10mic}	-	Temperature effects on microbial metabolic activity (rate change per 10 °C increase in temperature). Based on 0.65 eV activation energy for soils	[1.5, 3.5]	He et al. (2015)
Q_{10enz}	-	Temperature effects on enzyme activity (rate change per 10 °C increase in temperature). Based on 6% rate increase per degree Celsius	1.79	He et al. (2015)
$\boldsymbol{\alpha}$	-	the ratio of m_R to the sum of maximum specific growth rate	[0.01, 0.5]	Wang et al. (2014)
β	-	Ratio of dormant microbial maintenance rate to m_R	[0.0005, 0.005]	Wang et al. (2014)
Y_g	-	carbon use efficiency	[0.3, 0.7]	He et al. (2015)
K_s	mgC cm^{-2}	Half-saturation constant for directly accessible substrate	[0.01, 10]	Wang et al. (2014)
Km_{uptake}	mgC cm^{-2}	Half-saturation constant for enzymatic decay of SOC	[200, 1000]	He et al. (2015)
r_{death}	h^{-1}	Potential rate of microbial death	[$2e^{-4}$, $2e^{-3}$]	Allison et al. (2010)
$r_{EnzProd}$	h^{-1}	Enzyme production rate of microbe	[$1e^{-4}$, $8e^{-4}$]	He et al. (2015)
$r_{enzloss}$	h^{-1}	Enzyme loss rate	[0.0005, 0.002]	Allison et al. (2010)
V_{max}	mgC cm^{-2} h^{-1}	Maximum SOC decay rate	[$1e^{-4}$, $5e^{-3}$]	He et al. (2015)

Table 2. Site description and measured NEP data used to calibrate MIC-TEM-dormancy

Site Name	Location (Longitude (degrees) /Latitude (degrees))	Elevation (m)	Vegetation type	Description	Data range	Citations
Univ. of Mich. Biological Station	84.71W 45.56 N	234	Temperate deciduous forest	Located within a protected forest owned by the University of Michigan. Mean annual temperature is 5.83°C with mean annual precipitation of 803mm	01/2005-12/2006	Gough et al. (2013)
Howland Forest (main tower)	68.74W 45.20N	60	Temperate coniferous forest	Closed coniferous forest, minimal disturbance.	01/2004-12/2004	Davidson et al. (2006)
UCI-1964 burn site	98.38W 55.91N	260	Boreal forest	Located in a continental boreal forest, dominated by black spruce trees, within the BOREAS northern study area in central Manitoba, Canada.	01/2004-10/2005	Goulden et al. (2006)
KUOM Turfgrass Field	93.19W 45.0N	301	Grassland	A low-maintenance lawn consisting of cool-season turfgrasses.	01/2006-12/2008	Hiller et al. (2011)
Atqasuk	157.41W 70.47N	15	Wet tundra	100 km south of Barrow, Alaska. Variety of moist-wet coastal sedge tundra, and moist-tussock tundra surfaces in the more well-drained upland.	01/2005-12/2006	Oechel et al. (2014);
Ivotuk	155.75W 68.49N	568	Alpine tundra	300 km south of Barrow and is located at the foothill of the Brooks Range and is classified as tussock sedge, dwarf-shrub, moss tundra.	01/2004-12/2004	McEwing et al. (2015)

1022 **Table 3. Site description and measured NEP data used to validate MIC-TEM-dormancy**

1023

Site Name	Location (Longitude (degrees) /Latitude (degrees))	Elevation (m)	Vegetation type	Description	Data range	Citations
Bartlett Experimental Forest	71.29W/ 44.06N	272	Temperate deciduous forest	Located within the White Mountains National Forest in north-central New Hampshire, USA, with mean annual temperature of 5.61 °C and mean annual precipitation of 1246mm.	01/2005-12/2006	Jenkins et al. (2007); Richardson et al. (2007);
Howland Forest (main tower)	68.74W/ 45.20N	60	Temperate coniferous forest	Closed coniferous forest, minimal disturbance.	01/2003-12/2003	Davidson et al. (2006)
UCI-1964 burn site	98.38W/ 55.91N	260	Boreal forest	Located in a continental boreal forest, dominated by black spruce trees, within the BOREAS northern study area in central Manitoba, Canada.	01/2002-12/2003	Goulden et al. (2006)
Brookings	96.84W/ 44.35N	510	Grassland	Located in a private pasture, belonging to the Northern Great Plains Rangelands, the grassland is representative of many in the north central United States, with seasonal winter conditions and a wet growing season.	01/2005-12/2006	Gilmanov et al. (2005)
Atqasuk	157.41W/ 70.47N	15	Wet tundra	100 km south of Barrow, Alaska. Variety of moist-wet coastal sedge tundra, and moist-tussock tundra surfaces in the more well-drained upland.	01/2003-12/2004	Oechel et al. (2014);
Ivotuk	155.75W/ 68.49N	568	Alpine tundra	300 km south of Barrow and is located at the foothill of the Brooks Range and is classified as tussock sedge, dwarf-shrub, moss tundra.	01/2005-12/2005	McEwing et al. (2015)

1024

Table 4. Site description and measured R_H data used to validate MIC-TEM-dormancy model

Site	Location (Longitude (degrees) /Latitude (degrees))	Elevation (m)	Vegetation type	Data range	Citations
US-EML	149.25W/ 63.88N	700	Alpine tundra	01/2009-12/2013	Belshe et al. (2012)
CA-SJ2	104.65W/ 53.95N	580	Boreal forest	01/2004-12/2008	Coursolle et al. (2006)
US-Ho2	68.75W/ 45.21N	91	Temperate coniferous forest	01/2000-12/2004	Davidson et al. (2006)
US-UMB	84.71W/ 45.56N	234	Temperate deciduous forest	01/2005-12/2006	Gough et al. (2013)
US-Ro4	93.07W/ 44.68N	274	Grasslands	01/2016-12/2017	Griffis et al. (2011)
RU-Che	161.34E/ 68.61N	6	Wet tundra	01/2002-12/2005	Merbold et al. (2009)

Table 5. Model validation statistics for Dormancy model and MIC-TEM at six sites with NEP data

Site Name	Vegetation type	Models	Intercept	Slope	R-square	Adjusted R-square	p-value
Ivotuk	Alpine tundra	MIC-TEM	0.85	0.83	0.70	0.67	<0.001
		Dormancy	-0.51	1.09	0.75	0.73	<0.001
UCI-1964 burn site	Boreal forest	MIC-TEM	0.18	1.03	0.912	0.9080	<0.001
		Dormancy	-0.21	0.96	0.90	0.894	<0.001
Howland Forest (main tower)	Temperate coniferous forest	MIC-TEM	7.29	0.72	0.85	0.83	<0.001
		Dormancy	0.27	1.05	0.89	0.88	<0.001
Bartlett Experimental Forest	Temperate deciduous forest	MIC-TEM	-6.05	0.91	0.944	0.941	<0.001
		Dormancy	-2.34	1.13	0.93	0.924	<0.001
Brookings	Grassland	MIC-TEM	3.05	0.71	0.84	0.83	<0.001
		Dormancy	0.17	0.95	0.90	0.898	<0.001
Atqasuk	Wet tundra	MIC-TEM	7.22	1.85	0.71	0.70	<0.001
		Dormancy	0.19	0.82	0.67	0.66	<0.001

1055 **Table 6. Model validation statistics for Dormancy model and MIC-TEM at six sites with R_H data**
1056

Site ID	Vegetation type	Models	Intercept	Slope	R-square	Adjusted R-square	RMSE	p-value
US-EML	Alpine tundra	MIC-TEM	2.90	0.91	0.79	0.78	3.55	<0.001
		Dormancy	1.81	0.74	0.87	0.85	2.69	<0.001
CA-SJ2	Boreal forest	MIC-TEM	7.59	1.12	0.84	0.83	9.8	<0.001
		Dormancy	2.6	0.74	0.86	0.85	3.97	<0.001
US-Ho2	Temperate coniferous forest	MIC-TEM	4.07	0.89	0.86	0.84	12.39	<0.001
		Dormancy	6.59	0.71	0.91	0.89	11.83	<0.001
US-UMB	Temperate deciduous forest	MIC-TEM	-4.73	1.32	0.81	0.8	20.05	<0.001
		Dormancy	13.6	0.67	0.85	0.84	12.94	<0.001
US-Ro4	Grassland	MIC-TEM	9.34	0.87	0.81	0.79	11.25	<0.001
		Dormancy	4.81	0.65	0.86	0.84	9.21	<0.001
RU-Che	Wet tundra	MIC-TEM	2.5	0.67	0.72	0.71	6.24	<0.001
		Dormancy	1.96	0.77	0.81	0.79	5.95	<0.001